REPORT

OF

PORT AND HARBOUR TECHNICAL RESEARCH INSTITUTE

REPORT No. 2

An Experimental Study of Development
of Wind Waves

by

Tokuichi Hamada

June 1963

PORT AND HARBOUR TECHNICAL RESEARCH INSTITUTE
MINISTRY OF TRANSPORTATION

162 Kawama Yokosuka-City Kanagawa-Prefecture, Japan

Erratum

Page	Line	Error	Corrected
3	26	1958	1959
14	Figure in	Fig-9-1	should be replaced by the Figure in Fig-9-2
14	Figure in	Fig-9-2	should be replaced by the Figure in Fig-9-3
15	Figure in	Fig-9-3	should be replaced by the Figure in Fig-9-1
26	26	celeritry	celerity
32	7	have	here
35	34	as follows in	as follows; in

An experimental study of development of wind waves

Tokuichi Hamada*
Akihiko Shibayama
Hajime Kato

Contents

* Chief of Hydraulic Laboratory.

1. Introduction

The problem of the development of water waves by wind has still many ambiguous points. These ambiguities are caused by the complexities of phenomena, and physically the interaction of surface waves and air flow and occurrence of breaking of waves are reserved as difficulties for the understanding of the accurate mechanism of wave development. At the present the comprehensive computations are presented by O. M. Phillips (1957) and J. W. Miles (1957, 1960, 1962) (improved in some points by T. B. Benjamin (1959)) for the explanation of the linear interaction of waves and air flows, and the treatment of J. W. Miles has been received as a gool interpretation of physical phenomena (M. J. Lighthill (1962)). His theory is a linearized instability one which is similar to the computation of hydrodynamic instability of parallel shear flow.

O. M. Phillips (1958) suggested f^{-5}law as the rule of the intensity of energy spectrum of water surface profiles under wind action, when the equilibrium condition of energy balance is established. This law is considered suitable to apply to the high frequency zone of the surface spectrum. This simple expression includes the effect of the nonlinear surface condition as energy transfer of breaking and some interaction phenomena. The linear treatment of J. W. Miles can be used to the wind effect also upon the high frequency zone of wave spectrum. Turning backward, there has been a famous theory of H. Jeffreys (1925. 1926), which has not been so concrete as Miles' paper, but possible to include general lift effect of air flow. By the way the formulation of the problem concerned to high frequency components of wind wave spectrum is very complicated one and is reserved for future studies.

O. M. Phillips (1960) computed the mutual interaction of different frequency components of surface waves introduced through the nonlinear physical condition of free surface. His computation is for the calm air condition, and seems possible to be extended to the analysis of wind wave. The influence of this interaction may be significant in the high frequency zone in which breaking of waves is more or less promising. The energy of high frequency waves may be transported to lower frequency zone, and, if this is not so small, the motion of waves should be treated three-dimensionally. The problem is also resesved for the future.

On the other hand, concerned to the air flow on waves, the reasonable profile of mean wind velocity on wavy boundaries is not yet determined. In a two-dimensional problem, T. B. Benjamin (1959) made computations in the assumption of a few noperturbed velocity distributions of air flow over a wavy boundary. This may be reasonable when the degree of perturbation is small. But, if the wave height is finite, the experiment given by Von H. Motzfeld (1937) shows that the phenomenon is more complicated even in a case of stationary wavy forms. One more problem is

of direction of wavy boundary. Slight difference of the direction of propagation of component wave is sufficient to make short crest surface phenomena, and they cover the water surface irregularly, although each component wave can be treated as a long crest wave. So the three-dimensional treatment of air flow may be desirable.

We have these unsolved problems and decisive conclusions are not expectable. But, generally speaking, the progress of theories concerned to this problem is conspicuous since 1957. In this experiment, which has its commencement in April of 1962, we may generally proceed along the physical interpretation of the problem given by recent theories, and only in cases when this method is insufficient, our new suggestions will be referred. As the problem is very difficult, this moderatism of analysis is appropriate.

For the examination of the properties of wind waves, we used the frequency spectrum of measured wavy profile of water surface. Similar spectrums are already expressed by some authors. They are S. W. O. P. group (1957) and J. Dairbyshire (1959) for the observation of actual ocean, and R. W. Burling (1959) and B. Kinsman (1961) for the measurement of pond of small fetches. The method of directional spectrum published by S. W. O. P. can not be used in the experiment of our narrow air-water tunnel, and the direct method of frequenty spectrum is adopted. The method of spectrum analysis is of electric analogue type which is firstly presented by W. J. Pierson, Jr (1954) and S. S. Chang (1955). Our experiment belongs to a case in which the fetch is small and the wind velocity is large, and we have not yet found any paper concerned to similar cases. Therefore we are obliged to compare our experimental results with the field data of R. W. Burling (1959) and B. Kinsman (1961), and we hope that some other experimental data are informed to us. L. J. Tick (1959) computed two-dimemsionally the second order nonlinear component of frequency spectrum of surface waves, and then W. J. Pierson. Jr (1958) gave some interpretation of this nonlinear effect. Although the computation of L. J. Tick is concerned to the calm air condition, this effect is perceived significantly in our experiment of wind waves.

2. Experiment

2-1 General description

The waterway used in this experiment is covered by a wind tunnel and the wind wave can be generated on water surface by the uni-directional air flow artificially supplied into the tunnel. At the windward end of the waterway a mechanical wave generator is equiped to generate regular waves of relatively long period, and water in the waterway can be circulated to investigate the wind wave on the flowing water. Therefore we may study the problem of wind wave development in relatively comp-

licated circumstances by making use of the waterway, and as the first step of the investigation here we treat the development of wind waves caused by uni-directional steady air flow on still water. We call this experimental apparatus as the air-water tunnel. The tunnel has a part of uniform cross section in which the measurement is operated. The length of this part is 2850 cm. The cross section is 130 cm (height) × 150 cm (width). In the present experiment the depth of water is taken to 50 cm (the height of air flow is 80 cm), and measured wind waves are generally treated as deep water waves. The leeward end of this uniform part is widened smoothly to the width of 500 cm. At the final end of this enlarged part, air flow is blown out and surface waves are dissipated by wave dissipator. A axial wind blower is situated to the windward side of the uniform part and is driven by 75 H. P. (at 1250 r. p. m.) electric motor. The revolution number of the blower is controled from 125 r. p. m. to 1250 r. p. m,. Between the air blower and the uniform part for measurement there are guide walls and a fine grid for the purpose of the exclusion of influences of large scale turbulence and of the secondary flow produced by the air blower.

The general view of the part of the apparatus for measurement is shown in Fig-1. The side walls of this part are consisted of clear glass plates and the plysical

Fig-1 General view of experimental waterway.

condition in the tunnel can be perceived. The glass plates are figured by the straight latticework at intervals of 5 cm. The measurements of wind velocity and wave profile have been done in several cross sections. These sections are virtually named

according to the distance from the air inlet section. Here the air inlet section means the section where air flow initially contacts with the water surface. The sections for the measurement of wind velocity are A_a Section (65 cm distant from the air inlet), B_a Section (965 cm 〃), C_a Section (1865 cm 〃) and D_a Section (2765 cm 〃). The sections for the measurement of wave profiles are A_w Section (75 cm distant from the air inlet), B_w Section (975 cm 〃), C_w Section (1875 cm 〃), D_w Section (2775 cm 〃), and auxilliary C_w-1 Section (leeward side of C_w Section, 232 cm distant from C_w Section, C_w-2 Section (〃 , 452 cm 〃) and C_w-3 Section 〃 , 668.5 cm 〃).

We used pitot tubes of Prandtle type and a manometre of Göttingen type. The measurement of wind velocity at the height very near to the developed wavy surface was difficult, and in such cases the measurement was limited to the layer where the velocity fluctuation is fairly small. Wavy profile of water surface was measured by making use of the wave height metre of electric registance type, and, when direct profiles were necessary, they were recorded by ink writing oscillograph. During the experiment water was kept as clear as possible, and its temperature was in a range of 17°~26°C. In this wave height metre, the distance of two conductive bars immersed to water is 10.5 mm~16.2 mm, and so the metre is not proper to measure the high frequency capillary waves.

The electric spectrum analyzer for surface profiles was used to obtain the spectrum form of data. This apparatus is consisted of three parts. They are parts of (i) modulation and tape recording. (ii) mechanical speed-up and regeneration and (iii) analysis and recording. Tape-recorder is of pulse width modulation type, in which number of pulses is 150 per second. Desirable frequencies of input power is 1/4~20 $^c/_s$, and powers of higher frequencies are cutted off by low-pass filter. Tape speed is $1\frac{7}{8}$ inch/sec.. In the part of mechanical speed-up and regeneration. tape speed becomes forty times (75 inch/sec.), and so the range of wave number becomes to 10~800 c/sec.. The part of analysis is of heterodyne detection method. In brief, a local oscillator is active with the variation of its frequency linear to time and the current from this oscillator is coupled with the input current of 10~800 c/sec.. Then the compound current is orderly filtered by a crystal filter which has a central frequency of 10 K.C./sec., and the band width of the filter is only ±1 c/sec. and ±2 c/sec.. After the linear detection each frequency component of input power is recorded by an ink-writing ossillograph. The linear detection is adopted because it is more reliable than the square detection. Obtained records are corrected by the factor of linearity and then squared to the power. Fig-2 is a appearance of this analyzer. The magnetic tapere corder, analyzer and the part of mechanical speed-up and regeneration are situated in turn from left to right.

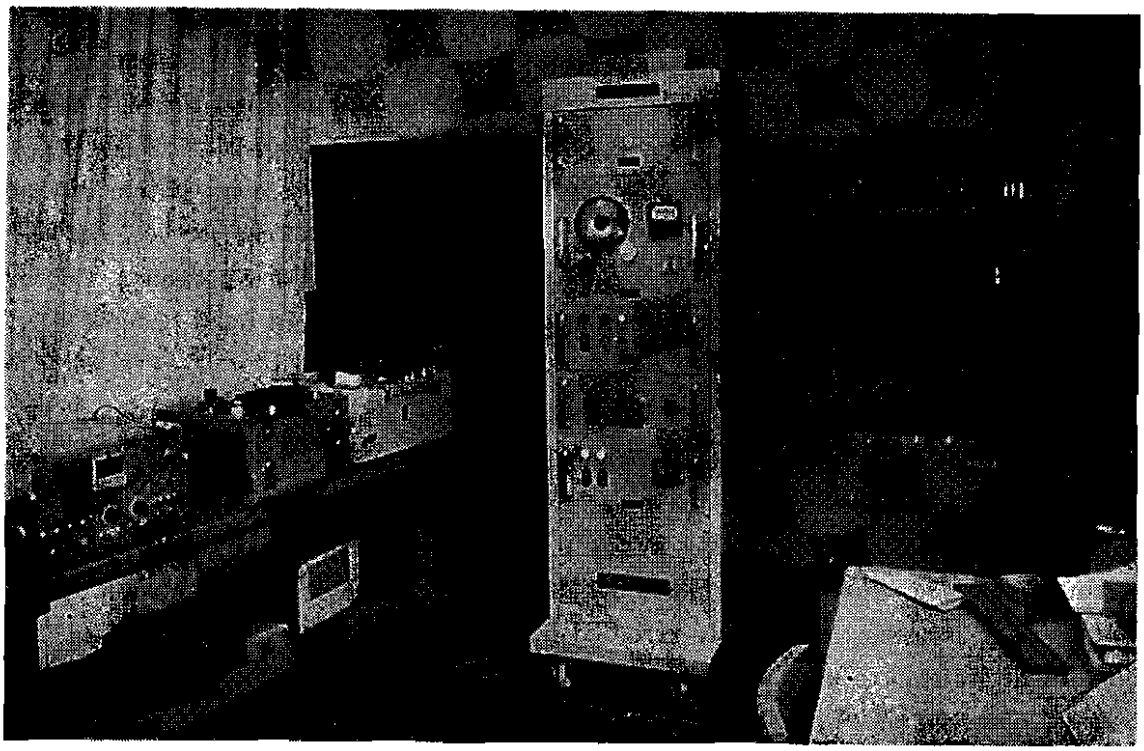

Fig-2 Spectrum analyzer.

2-2 General description of air flow

Air flow inflows fromthe inlet to the tunnel in a condition of almost uniform distribution of velocity, and in the tunnel generally boundary layers develop. Fig-3 shows one example of velocity distribution at A_a Cross Section (a case of 400 r.p.m. of blower), and the velocity is almost is a range of 1070 cm/sec.~1100 cm/sec.. The velocity of upper layer is slightly large, and through the middle and lower layer the velocity is rather uniform. Combining this result with the results in cases of 200 r.p.m. and 400 r.p.m. of blower. the averaged wind velocity of A_a cross section may be related to the revolution number of blower, and is shown in Fig-4. Within the range of this measurement, the averaged velocity is linear to r.p.m. of blower.

Concerned to B_a and C_a Cross Section, the velocity distributions along the mid-stream plane are shown in Fig-5 and Fig-6. They are vertical velocity distributions of cases of 200, 300 and 400 r.p.m. of blower. The development of boundary layers from both the water surface and the fixed wall of upper end may be easily noticed.

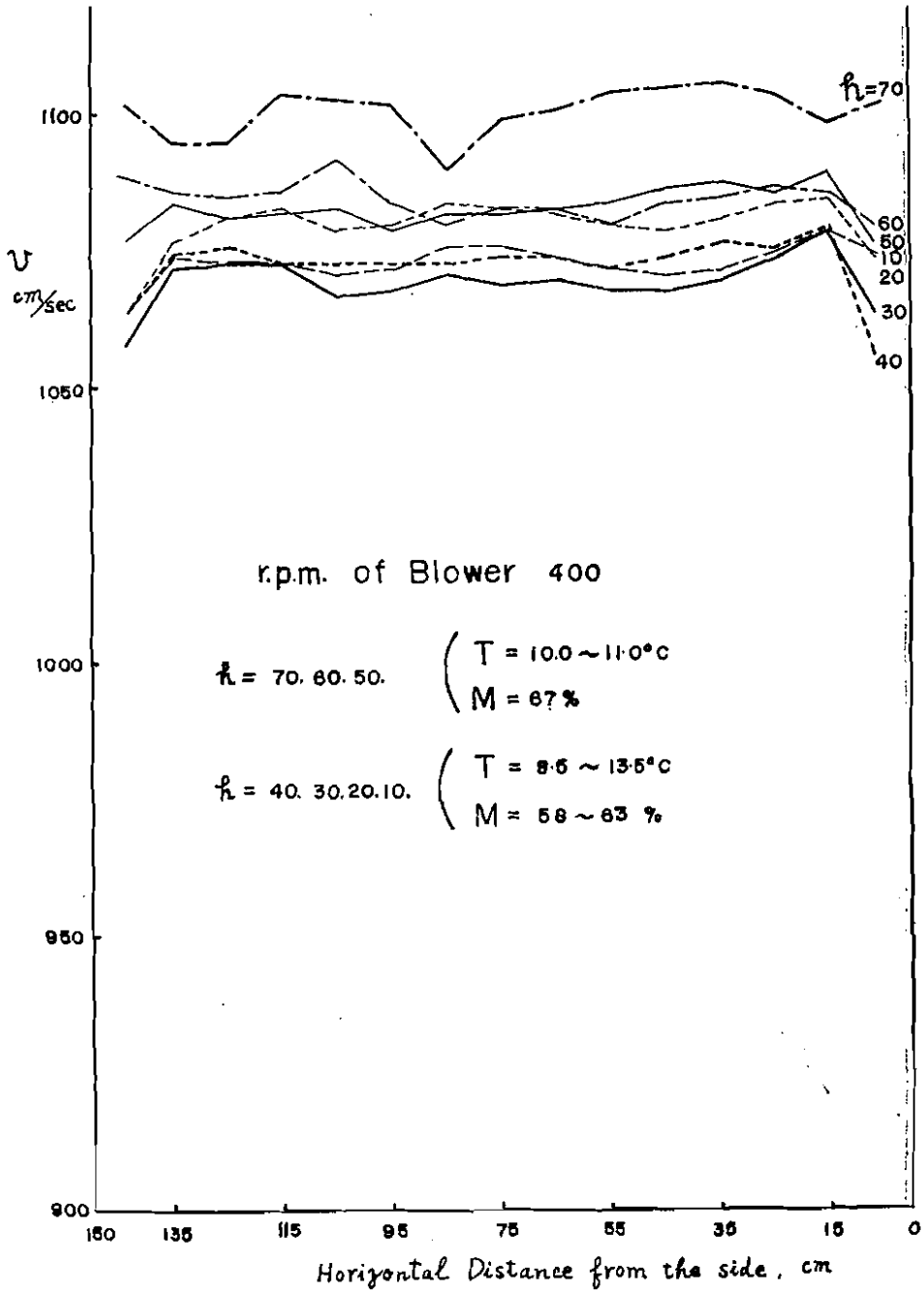

Fig-3 Distribution of Wind Velocity at A_a Section, each curve indicates the velocity profile at a fixed height.

h : the height above the mean water level (cm)

T : temperature of air (°C)

M : relative humidity (%)

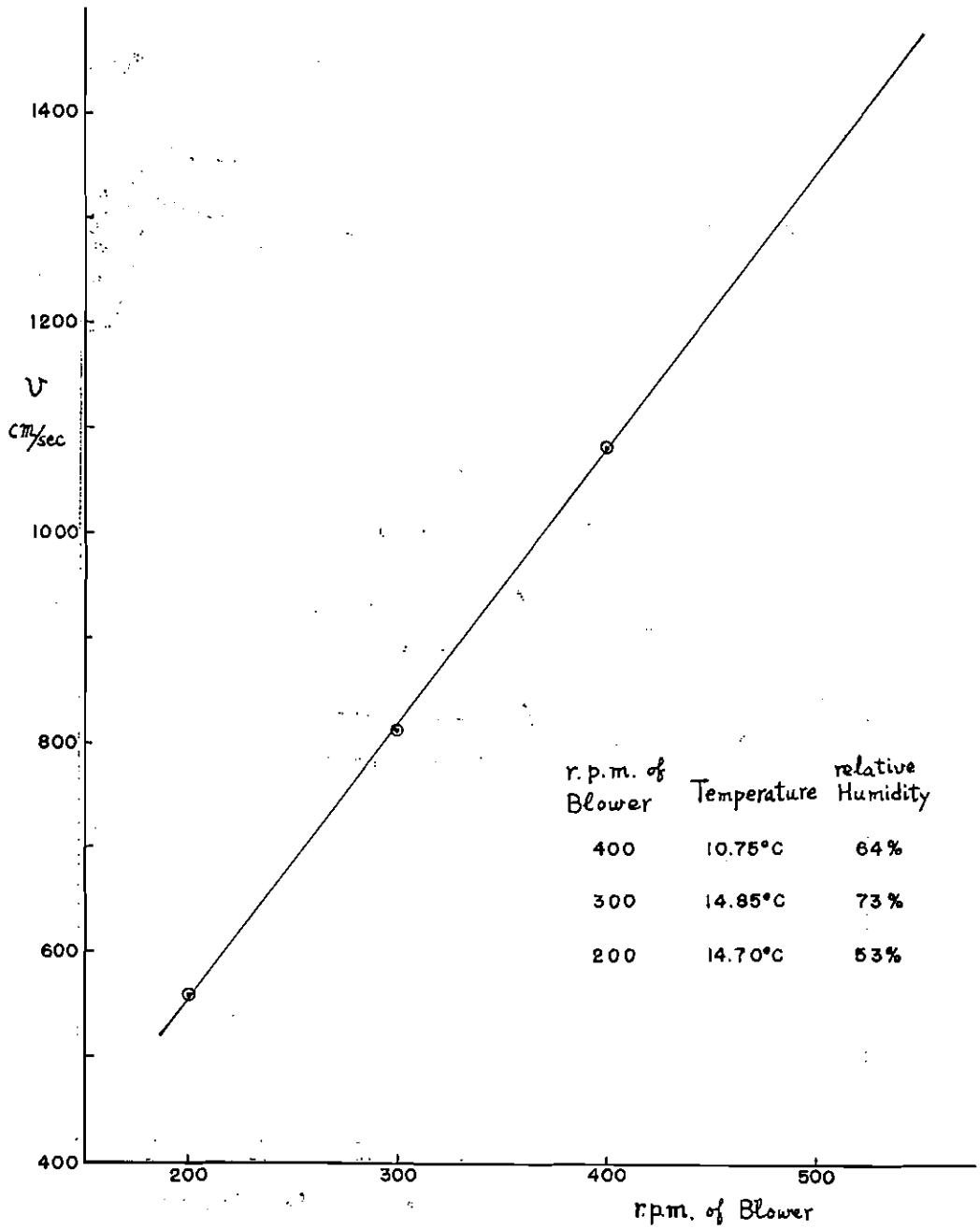

Fig-4 Averaged Wind Velocity related to ther. p. m. of Blower, A_a section.

depth of water 50 cm
total height of air flow 80 cm .

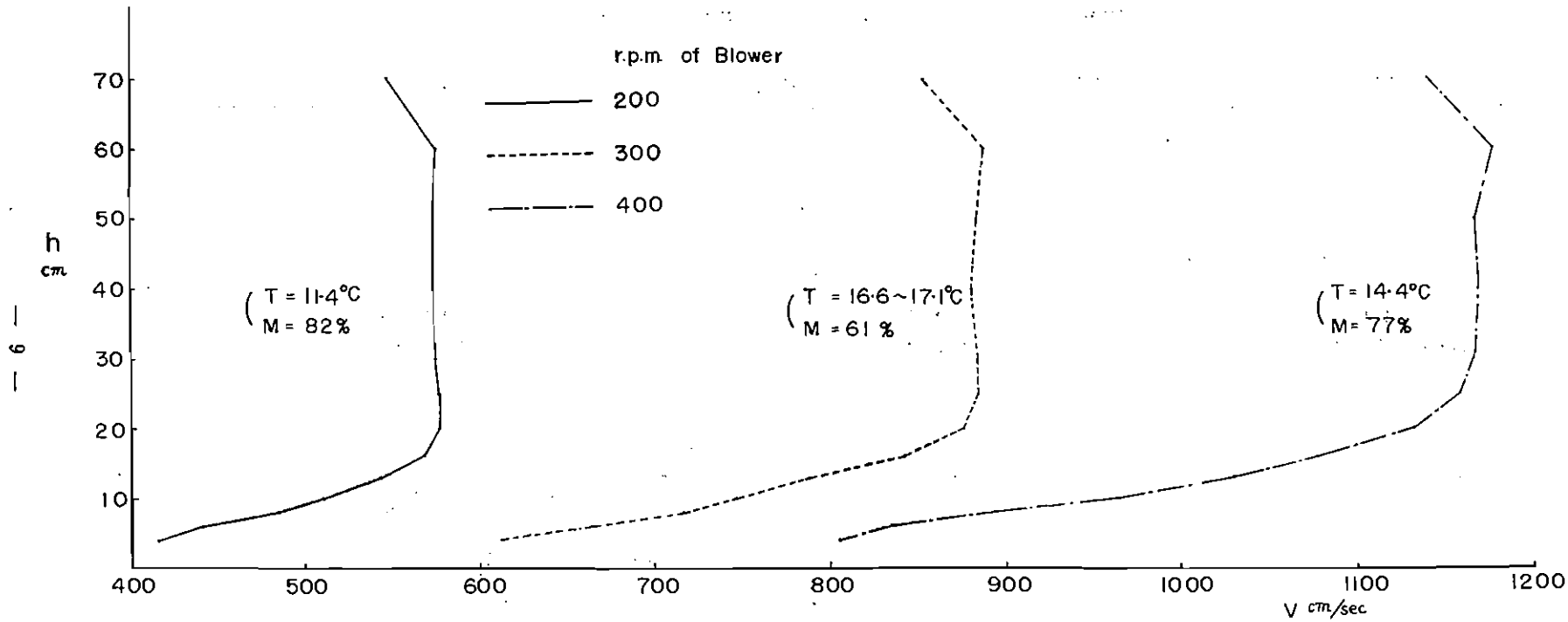

Fig-5 Velocity Distributions at the Midstream Plane, B_a Section.

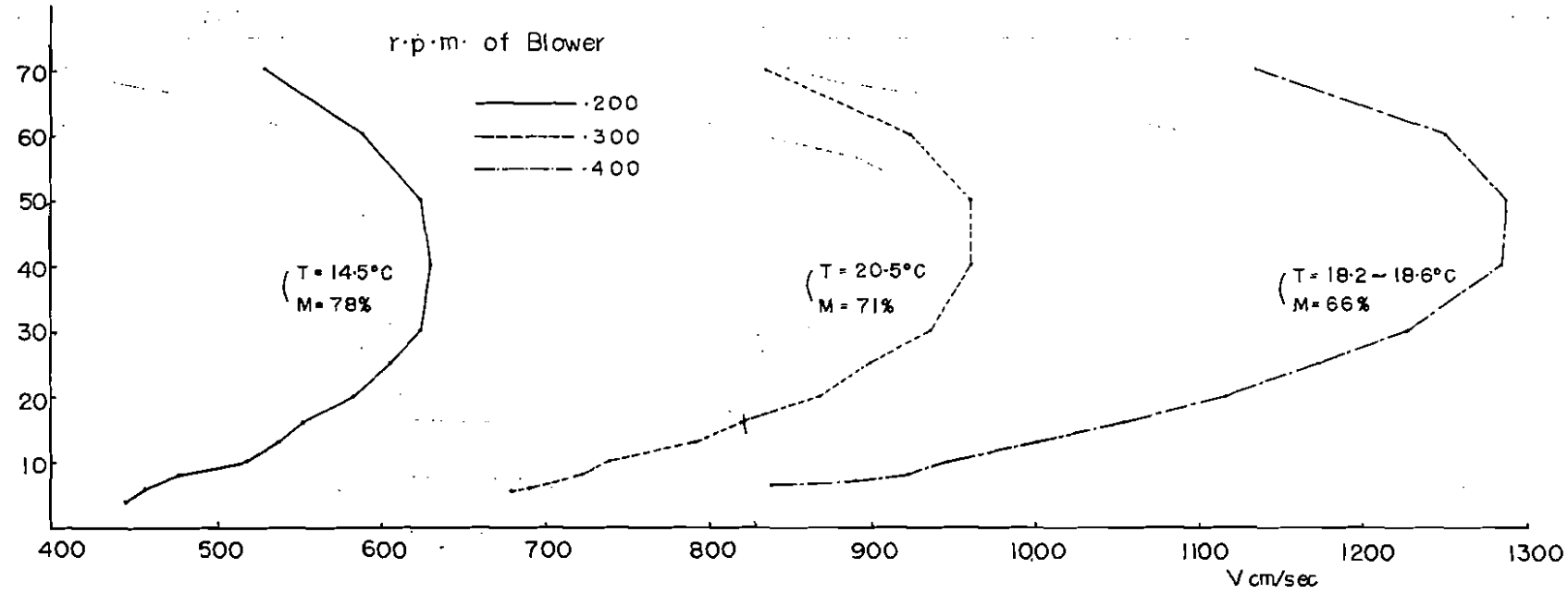

Fig-6 Velocity Distributions at the Midstream Plane, C_a Section.

In Da Cross Section, vertical velocity distributions along planes, which are in order 35 cm, 75 cm and 115 cm apart from the left hand side (facing to leeward) glass wall, are shown in Fig-7-1, Fig-7-2, Fig-7-3. Fig-7-1 is for 400 r.p.m. of blower, Fig-7-2 for 300 r.p.m., and Fig-7-3 for 400 r.p.m. Velocity distributions are a

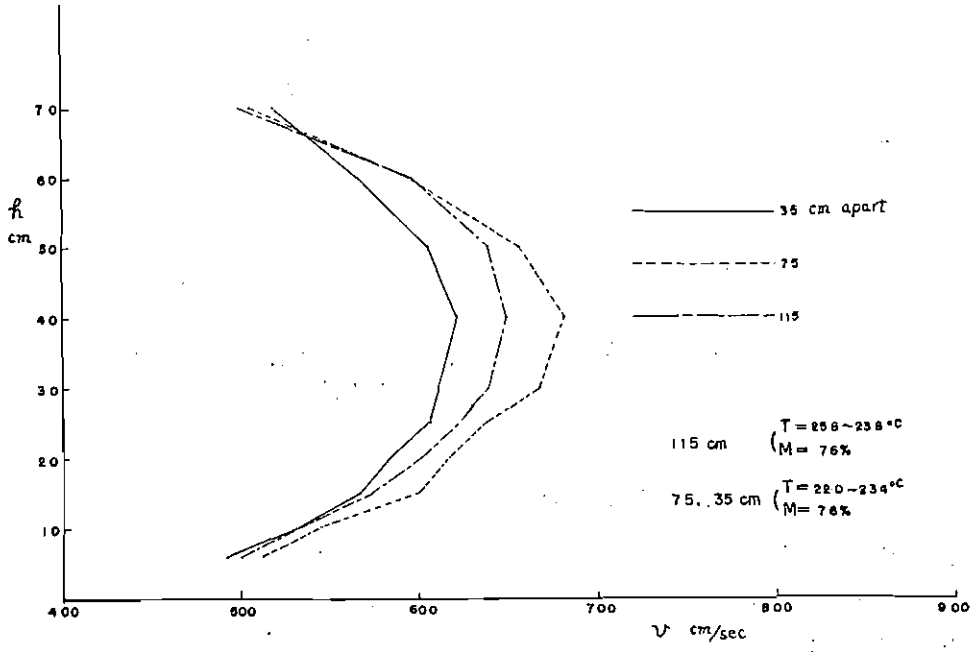

Fig-7-1 Vertical Distributions of Velocity, D_a Section, r.p.m. of Blower 200.

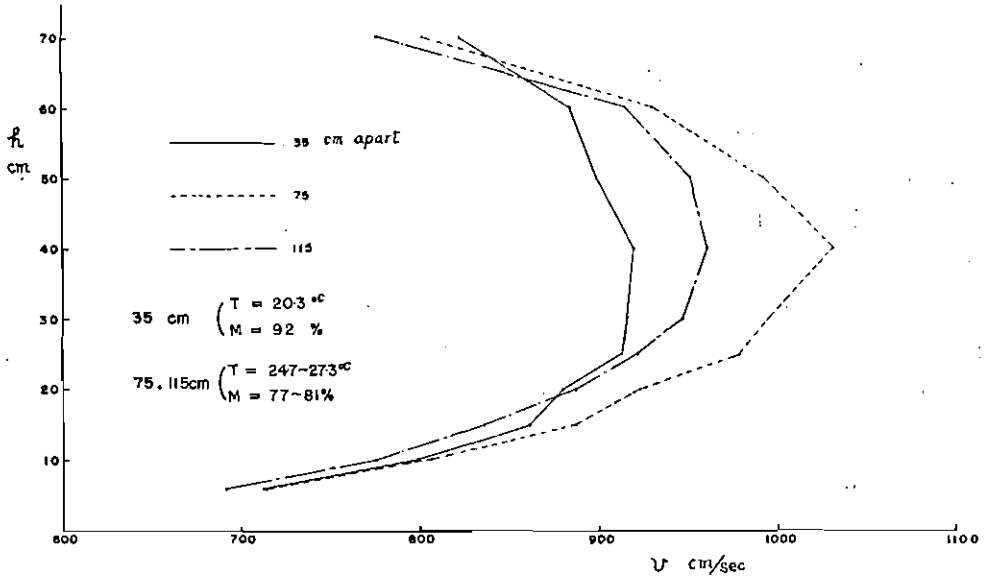

Fig-7-2 Vertical Distributions of Velocity, D_a Section, r.p.m. of Blower 300.

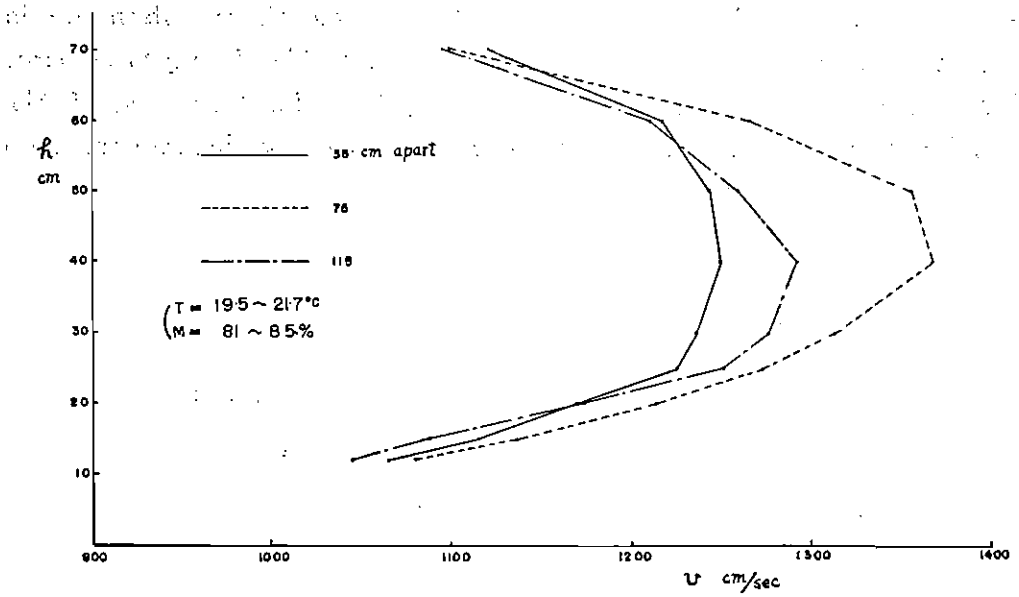

Fig-7-3 Vertical Distributions of Velocity, D_a Section, r. p. m. of Blower 400.

little asymmetric concerned to the middle plane, and at the height 40 cm above the water surface the velocity of 115 cm distant from left hand side wall is slightly greater than that of 35 cm distant from the same wall. In Fig-7-3 the wind velocity is not exactly measured below the horizontal plane 14 cm above the still water surface, and this inaccuracy is due to the strong perturbed air flow near wavy surfaces. The temperature and relative humidity of air in each measurement are shown in each figures.

2-3 General description of wave profile

In this experiment the change of mean water level caused by the wind shear is very small and can be neglected in the measmement of wind waves. To know the general characteristies of wave profile, the distribution of $\eta_{\max.}$ and $\eta_{\min.}$ from still water level was examined. $\eta_{\max.}$ means the each maximum point of wavy profile including cases when the addressed point situates below the still water level. $\eta_{\min.}$ are minimum points in the same meaning. The distribution of $\eta_{\max.}$ and $\eta_{\min.}$ thus defined was theoretically examined by M. S. Longuet-Higgns (1952) and D. E. Cartwright and M. S. Longuet-Higgins (1956), under the condition that the distance of instantaneons water level from the still water level is statistically distributed as gaussian, and here we only show actual distributions in our experiment without the detailed discussion.

We took about 500 waves in continuous and stationary condition. Wave height is virtually defined as the vertical distance of $\eta_{\max.}$ and $\eta_{\min.}$ in case when they

confine so called zero up-cross. Fig-8-1, 2, 3; Fig-9-1, 2, 3; and Fig-10-1,2, 3 are thus obtained. Fig-8-1, 2, 3 are read from the wave profile measured at the middle surface of C_w Cross Section at 200 r.p.m. of blower. Fig-9 and Fig-10 are due to the wave records of the same point at 300 and 400 r.p.m. of blower respectively. According to these figures the distributions of $\eta_{max.}$ are fairly different from those of $\eta_{min.}$, and the distribution of $\eta_{min.}$ is not agreeable with the theory of gaussian assumption. As we shall state later, this inconsistency is remarkable in the case of 400 r.p.m. of blower (in the case of high wind velocity), when the nonlinear component of power spectrum of surface profile is conspicuous.

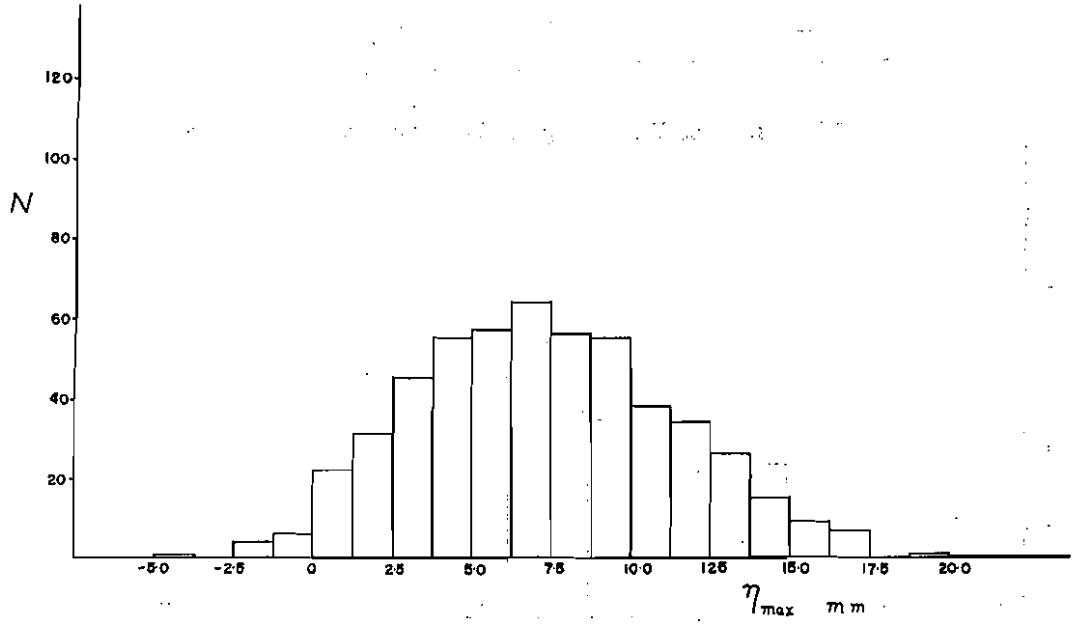

Fig-8-1 Distribution of η max, C_w Section, r.p.m. of Blower 200.

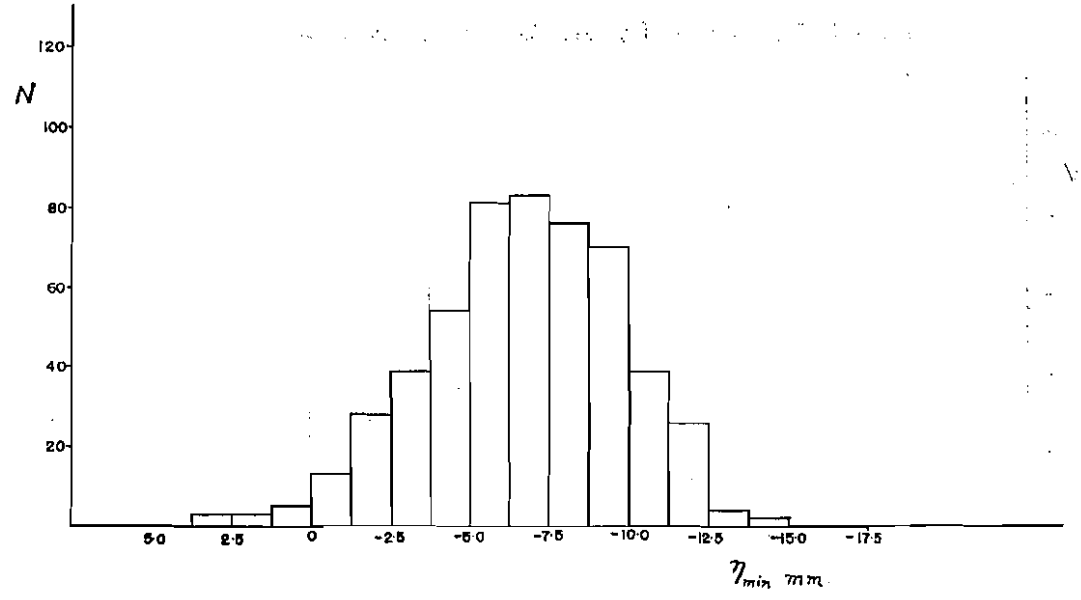

Fig-8-2 Distribution of η min, C_w Section, r.p.m. of Blower 200.

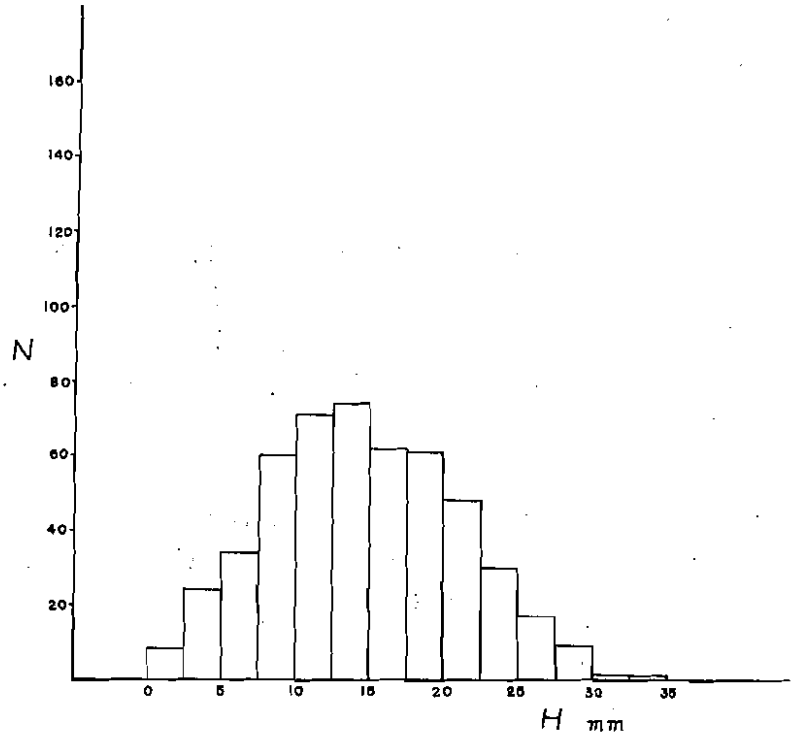

Fig-8-3 Distribution of Wave Height, C_w Section, r. p. m. of Blower 200.

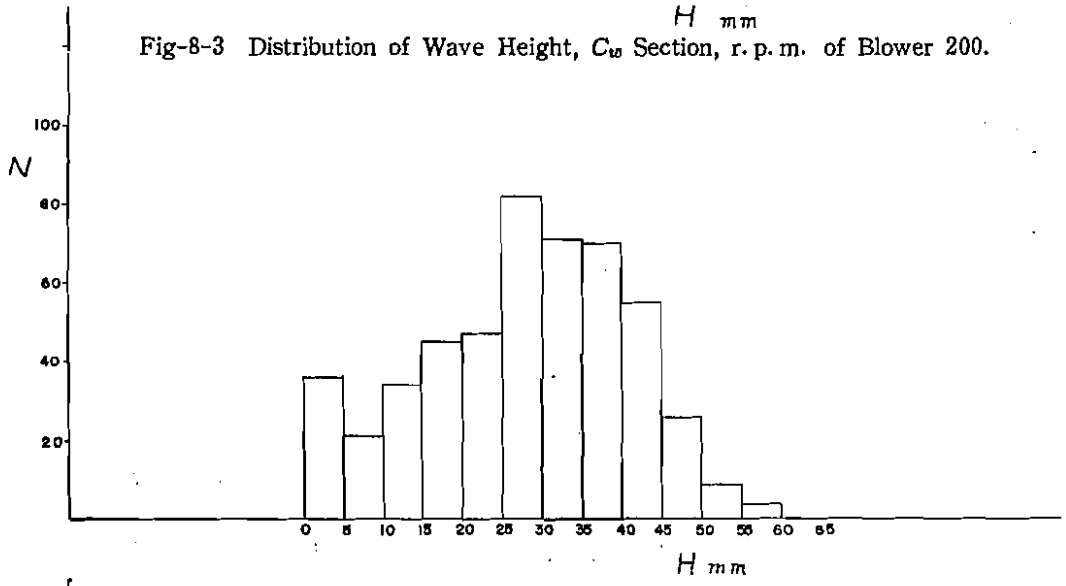

Fig-9-1 Distribution of η max, C_w Section, r. p. m. of Blower 300.

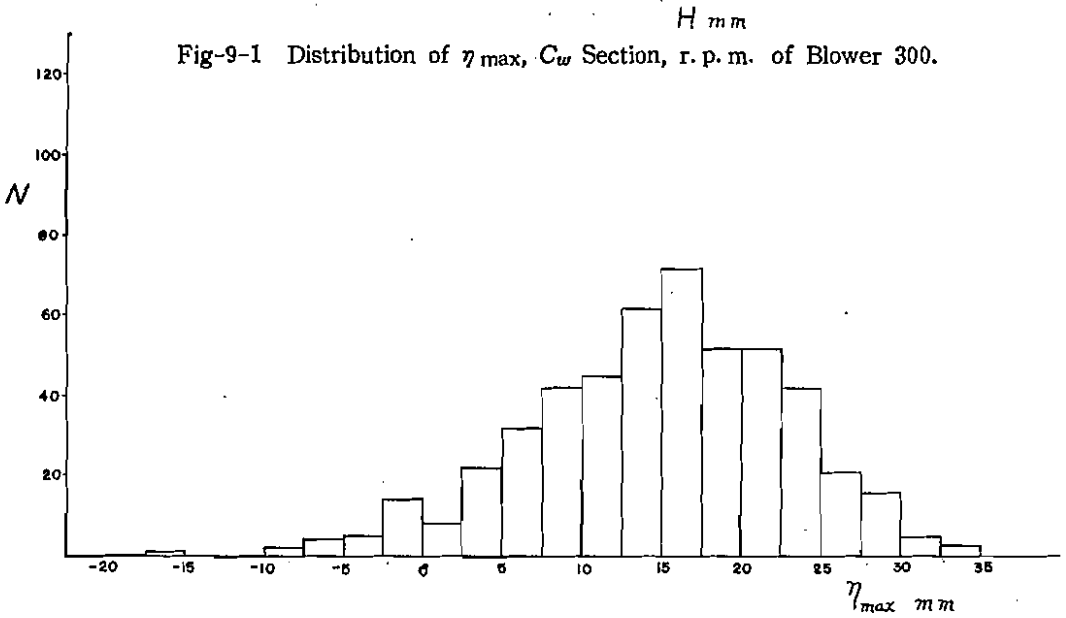

Fig-9-2 Distribution of η min, C_w Section, r. p. m. of Blower 300.

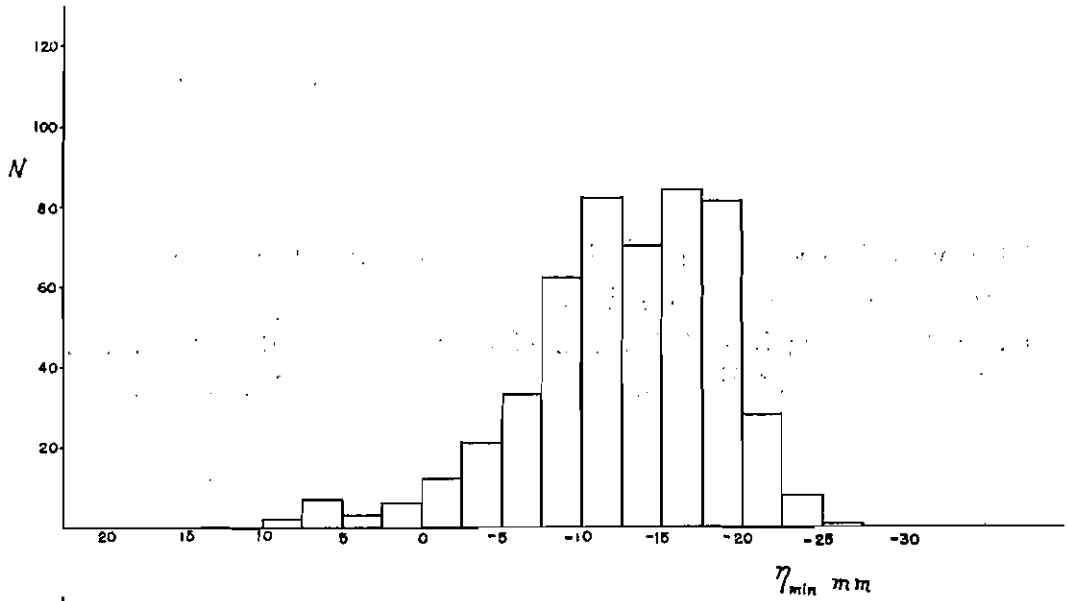

Fig-9-3 Distribution of Wave Height, C_w Section, r. p. m. of Blower 300.

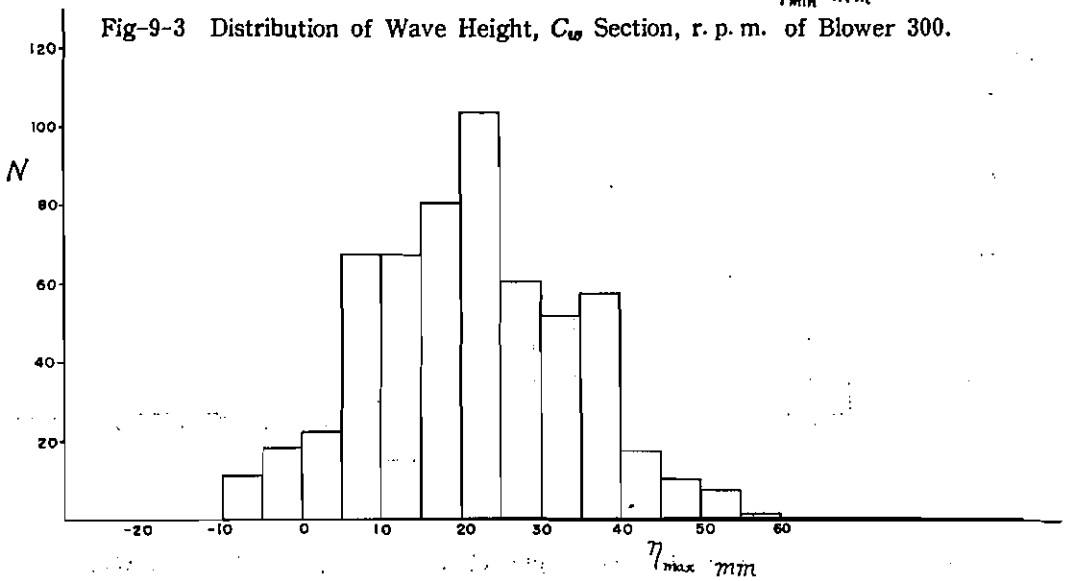

Fig-10-1 Distribution of η max, C_w Section, r. p. m. of Blower 400.

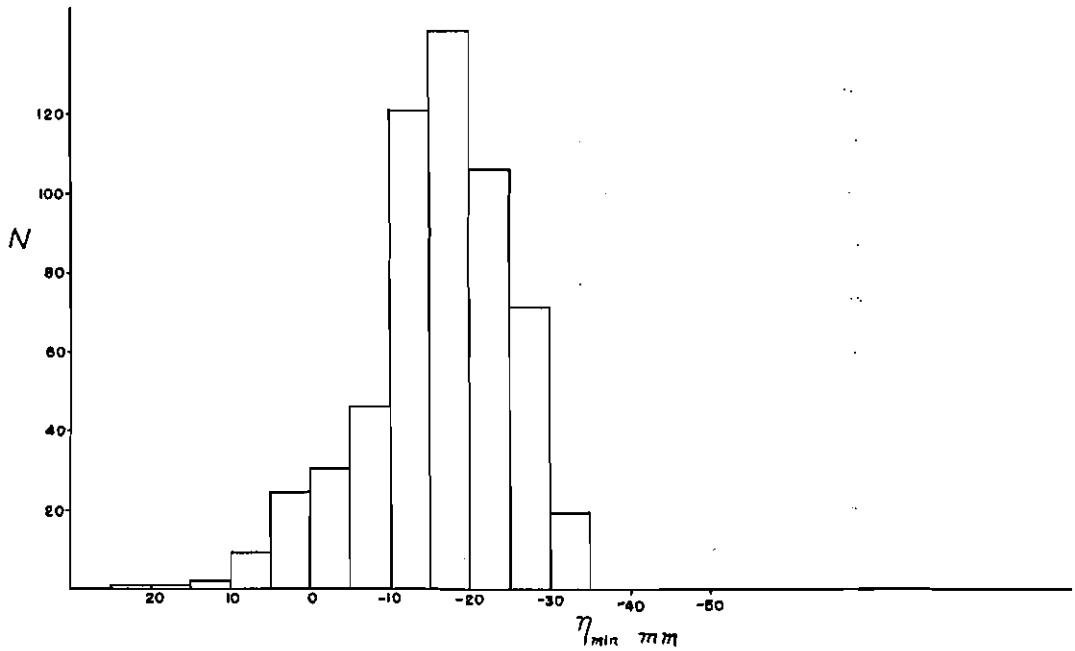

Fig-10-2 Distribution of η min, C_w Section, r. p. m. of Blower 400.

Then we define wave period $\tilde{T}$ by the time duration between neighbouring zero up-crosses, and its distribution can be shown similarly. Fig-11 corresponds to 200 r.p.m. of blower, Fig-12 to 300 r.p.m. of blower and Fig-13 to 400 r.p.m. of blower. The distribution of $\tilde{T}$ has almost same tendencies in these 3 figures.

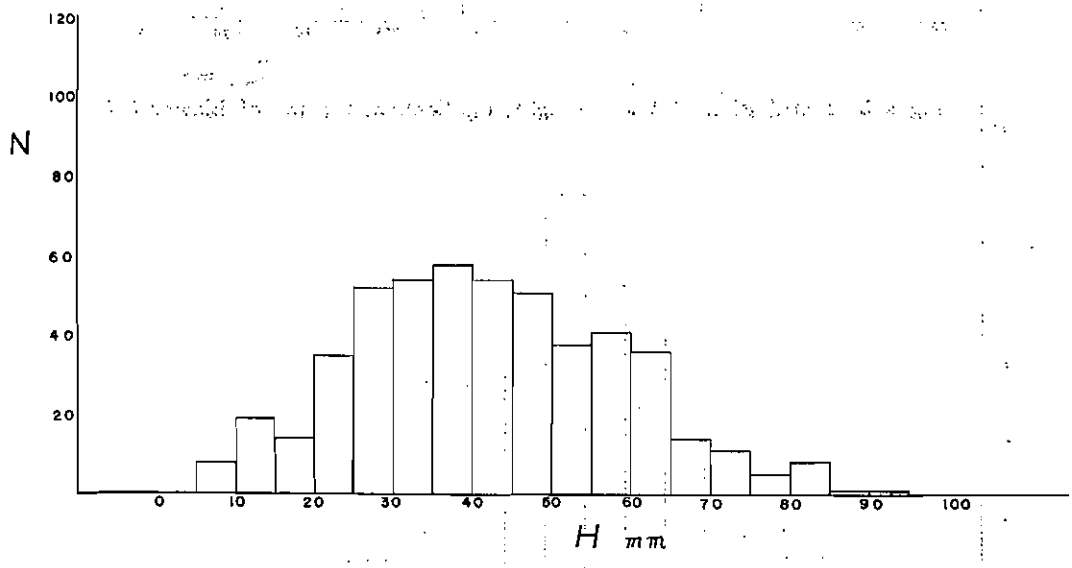

Fig-10-3 Distribution of Wave Height, C_w Section, r.p.m. of Blower 400.

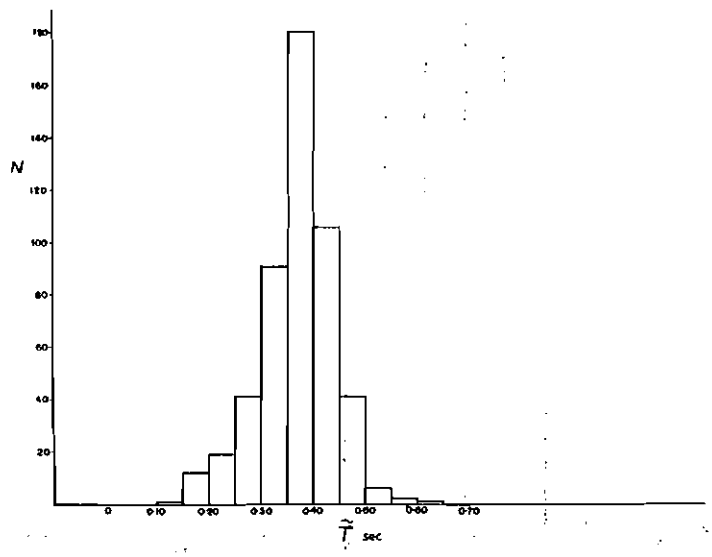

Fig-11 Distribution of Wave Period, C_w Section. r.p.m. of Blower 200.

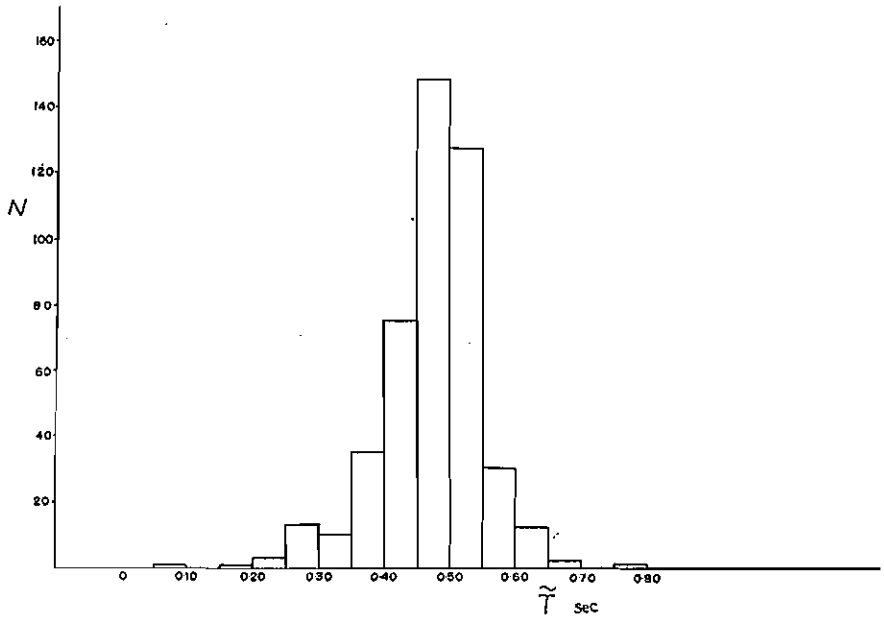

Fig-12 Distribution of Wave Period, C_{t0} Section, r.p.m. of Blower 300.

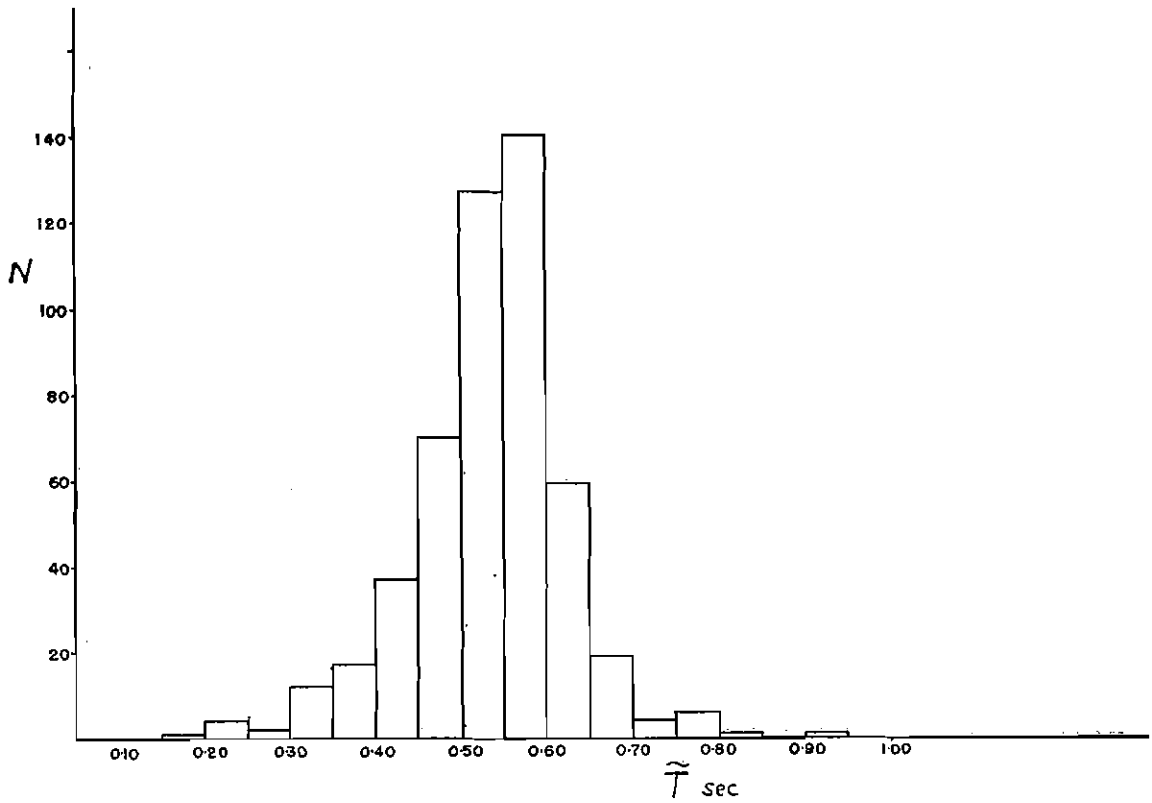

Fig-13 Distribution of Wave Period, C_{t0} Section, r.p.m. of Blower 400.

3 Analysis of experimental data

3-1 Confidential limit of spectrum

According to W. J. Pierson, Jr. (1954), the freedom of spectrum as x^2-distribution may be easily determined by the duration time of wave recording and shape of filter, if the assumption is made that the true intensity of spectrum is almost uniform through the range of frequency covered by filter. The shape of filter which we have used is shown in Fig-14 in the form of speed-up ratio of 40 times, and the recording time at one test has been 120 seconds. So simple computation shows that

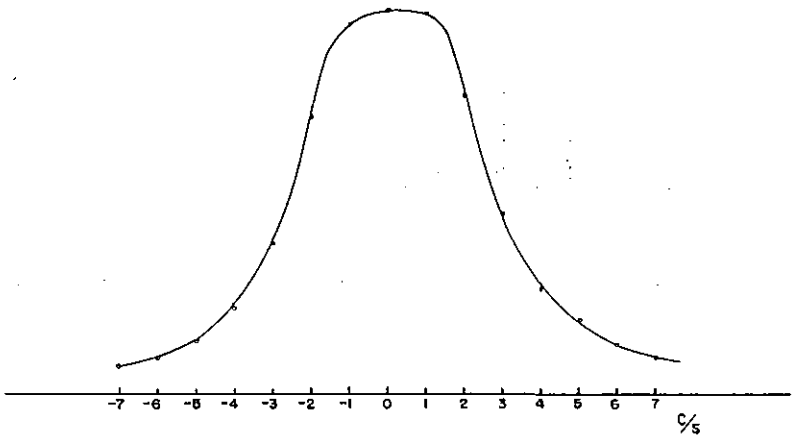

Fig-14 The Shape of Filter.

x^2-freedom of spectrum is $N=36$. This value of N is comparable to the value which is obtained in the 20 minutes continuous recording in actual ocean, and the greater value of N should be desirable in the test of experimental water way. Accordingly the average of 3 pieces of data is taken as the experimental value for the same stationary condition of experiment.

The x^2-freedom of each spectrum becomes 36×3, and, in the domain where the spectrum intensity is not so varied, $\frac{1}{K_{0.95}}=1.27$, $\frac{1}{K_{0.05}}=0.81$ (Notations due to W. J. Pierson, Jr. (1954)) may be obtained. Thus the resulted spectrum has relatively narrow 90% confidential limit.

3-2 Effect of the side wall

It is very difficult to discuss the influence of side wall upon surface spectrum theoretically, and here the experimental results are shown to know whether the homogeneity of wave spectrum in the lateral direction of tunnel is sustained or not in the stationary condition. In Fig-15 spectrums of C_w Cross Section at 300 r.p.m. of blower are obtained at (i) the centre of the section, (ii) 25 cm aside of the center and (iii) 50 cm aside of the centre. From this figure, we can find that the peak value of spectrum intensity of a point 25 cm aside the centre is low, and that the

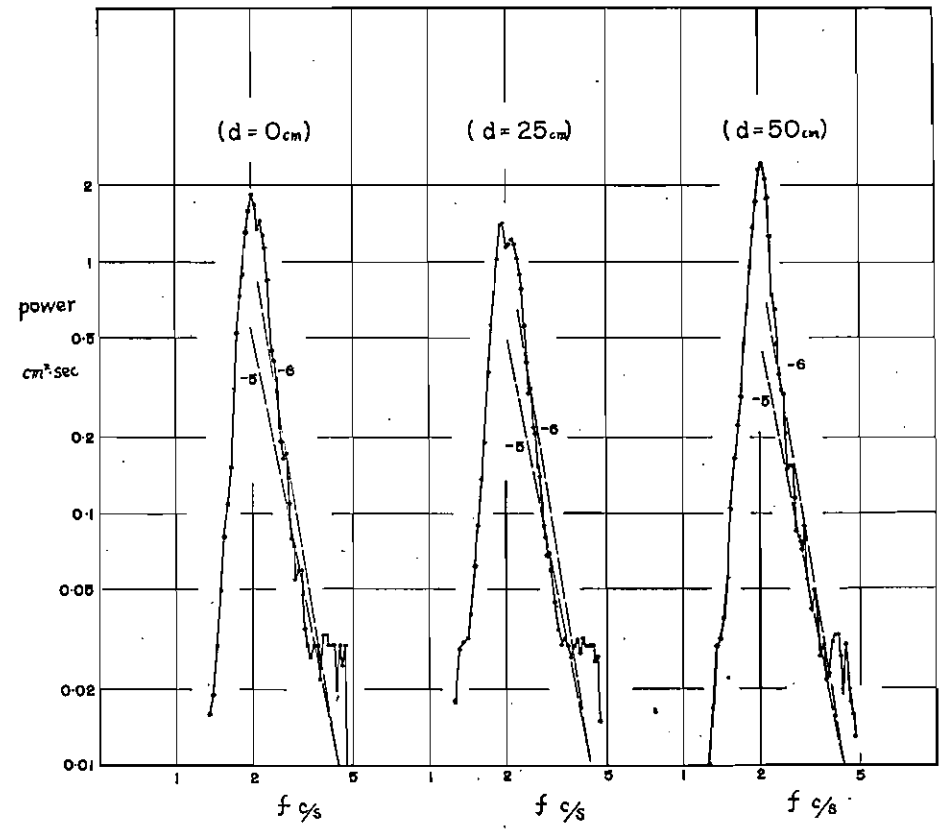

Fig-15 Spectrums at C_w Section, r.p.m. of Blower 300.

peak value of intensity of a point 50 cm aside the centre is high. The difference exceeds the 90% confidential limit each other. The intensity of the spectrum of the centre point situates in the middle of the above two spectrum. Homogeneity seems to be a little broken down by the finite width of the waterway. $\overline{\eta^2}=\int_0^\infty E(\omega)\,d\omega$ indicates 0.985 cm²(centre), 0.870 cm²(25 cm aside). 1.062 cm²(50 cm aside). $H_{1/3}$ by M. S. Longuet-Higgins (1952), assuming ε (the band width parametre of spectrum) $\to 0$, is 3.97 cm(centre), 3.73 cm(25 cm aside) and 4.12 cm(50 cm aside).

3-3 Physical properties of wind profile

In the theoretical treatment of development of surface waves, we need two types of stress. They are horizontal stress (x-direction from windward to leeward) and vertical stress (y-direction upwards positive). In the presence of wavy surface, these stresses may be transformed to the stress tangential to surface, and the stress normal to surface. In a case of linearized surface condition, the steady part of this tangential stress is considered to act on the drift current, and is generally neglected in the mechanism of wave development(J. W. Miles(1962)). In the presence of mass transport of waves, a rough estimation is given by R. W. Stewart(1961), but this by no means indicates that the steady tangential stress is effective firstly to the development of wind waves.

If the direction of wave progress is oblique to the direction of wind, the combination of the two-dimensional problem may be used (J. W. Miles (1960)).

The direct measurement of surface stresses is very difficult and our measurement is limited to that of wind velocity. According to the measured velocity profile, we may determine so called friction velocity and z_0. z_0 is the height (above mean water level) of a point where wind velocity becomes to zero in the assumed logarithmic profile. These two parametres may be used to investigate the property of non-negative damping factor of wave in a similar way to J. W. Miles (1957, 1960).

In the measurement of wind velocity by pitot tube, three regions can be vertically divided; (i) lower region where the measured velocity is greater than the velocity assumed by logarithmic profile of (ii), (ii) region where is almost accurately presented by logarithmic profile, (iii) upper region where the measured velocity is smaller than the assumed velocity by the extension of (ii). The friction velocity U_* and z_0 are determined with the assumption that the region expressed in (ii) may be extended to the direct water surface which is more or less roughened. Of course, the wind velocity sufficiently near to the wavy surface is disturbed by strong perturbed flow, and actual state has not been clarified in this experiment.

Table-1 and 〃-2 show obtained values of U^*, τ_0, z_0 and U_{10m}, U_{40cm}. Here U_{10m} means the assumed wind velocity at the height 10m above the mean water level, when the velocity distribution of logarithmic profile in the wind tunnel is extended to higher space, and U_{40cm} is the measured velocity at the height 40cm above the mean water level. (usually the maximum wind velocity appears at that height.)

Table-1 Characteristics of Air Flow

Section	r.p.m. of Blower	ρ_a	τ_0 dyne/cm²	U_* cm/sec	z_0 cm	U_{1000cm} cm/sec	U_{40cm} cm/sec	$z_0/H_{1/3}$	$H_{1/3}$cm
B_a	200	0.001240	3.19	50.72	0.178	1091	574	0.1155	1.54
B_a	300	0.001220	6.10	70.70	0.137	1578	880	0.0535	2.56
B_a	400	0.001220	11.13	95.53	0.179	2076	1168	0.0446	4.01
C_a	200	0.001242	2.21	42.21	0.081	998	631	0.0327	2.47
C_a	300	0.001214	5.80	69.13	0.136	1544	961	0.0331	4.10
C_a	400	0.001234	12.66	101.3	0.248	2115	1284	0.0397	6.24

In Table-1, observations were done on the midstream line at B_a and C_a Cross Section, and in Table-2 observations were done at three places of D_a Cross Section. These are at (i) midstream line, (ii) 40cm left to midstream line (L=35 cm) and (iii) 40cm right to midstream line (L=115 cm).

For the determination of average wind speed U in fetch graph and reference

velocity U_1 in the meaning of J. W. Miles (1957), wind velocity U_{10cm}, U_{40cm}, and shear velocity U_* are adjusted in B_a and C_a Cross Section after the average value of measurement of three places tn D_a Cross Section. This is not strict, but the adjusted values approach to the mean value of each cross section. In Table-1 and 〃-2, $z_0/H_{1/3}$ is also recorded. $H_{1/3}$ is pursued by energy spectrum of surface profile by the assump-

Table-2 Characteristics of Air Flow

Section	r.p.m. of Blower	L cm	ρ_a	τ_0 dyne/cm^2	U_* cm/sec	z_0 cm	U_{1000cm} cm/sec	U_{40cm} cm/sec	$z_0/H_{1/3}$	$H^1/_3$cm
D_a	200	35	0.001185	1.22	32.13	0.013	893	622		
D_a	200	75	0.001188	1.75	38.39	0.030	986	682	0.00864	3.47
D_a	200	115	0.001177	1.55	36.30	0.027	952	649		
D_a	300	35	0.001193	5.08	65.31	0.072	1540	920		
D_a	300	75	0.001180	5.72	69.65	0.097	1598	1031	0.01830	5.30
D_a	300	115	0.001180	4.79	63.75	0.076	1503	961		
D_a	400	35	0.001207	9.65	89.45	0.104	2046	1250		
D_a	400	75	0.001203	12.84	103.35	0.182	2218	1367	0.02363	7.70
D_a	400	115	0.001203	12.07	100.18	0.200	2162	1292		

tion of narrow band width ($\varepsilon \to 0$). $z_0/H_{1/3}$ may have two physical meanings. Firstly $z_0/H_{1/3}$ has the meaning comparable to ξ_c ($=k\,y_c$) (J. W. Miles (1957, 1960)) at the initial stage of wave development and is related closely to non-negative damping factor of wave development in the computation of J. W. Miles. Another meaning is that when wave height is treated as finite one, this quantity may be related to the grade of separation of air flow from wave profile, especially in our cases when C/U_1 is extremely small. As will be stated later, $z_0/H_{1/3}$ is efficiently related to non-negative damping factor in our experiment.

Table-3 shows γ^2 which is determined by the relation $\tau_0=\rho_a\gamma^2U^2$ (U is taken to U_{10m} and U_{40cm}) in Table-1 and 〃-2. The value of γ^2 is systematically changed in accordance with the magnitude of wind velocity at D_a Cross Section where the turbulent boundary layer along the water surface is sufficiently developed. This is same to the tendencies in many other wind-water tunnel experiments. The one cause of this change may be given by the change of wave height in contrast with the limited condition of height of air flow. In our experiment, in which c/U_1 is extremely small and water surface is covered by very steep waves, the change of wave height may be effective in some degree in the similar influence to the change of roughness height in turbulent pipe flow. On the other hand, if γ^2_{10m} at D_a Cross Section is compared with the value of field observation shown by Fig-3 of E. L. Deacon (1962), the absolute value is rather a little greater in our case, but the tendency of

Table-3 Values of γ^2

Section		r. p. m. of Blower	U_{1000cm} cm/sec	γ^2_{1000cm}	U_{40cm} cm/sec	γ^2_{40cm}
B_a		200	1091	0.00216	574	0.00780
〃		300	1578	0.00200	880	0.00645
〃		400	2076	0.00211	1168	0.00668
C_a		200	998	0.00178	631	0.00446
〃		300	1544	0.00200	961	0.00517
〃		400	2115	0.00229	1284	0.00622
D_a	L=35cm	200	893	0.00129	622	0.00266
〃	75cm	〃	986	0.00151	682	0.00316
〃	115cm	〃	952	0.00145	649	0.00312
D_a	L=35cm	300	1540	0.00179	920	0.00503
〃	75cm	〃	1598	0.00189	1031	0.00456
〃	115cm	〃	1503	0.00179	961	0.00440
D_a	L=35cm	400	2046	0.00191	1250	0.00512
〃	75cm	〃	2218	0.00217	1367	0.00571
〃	115cm	〃	2162	0.00214	1292	0.00601

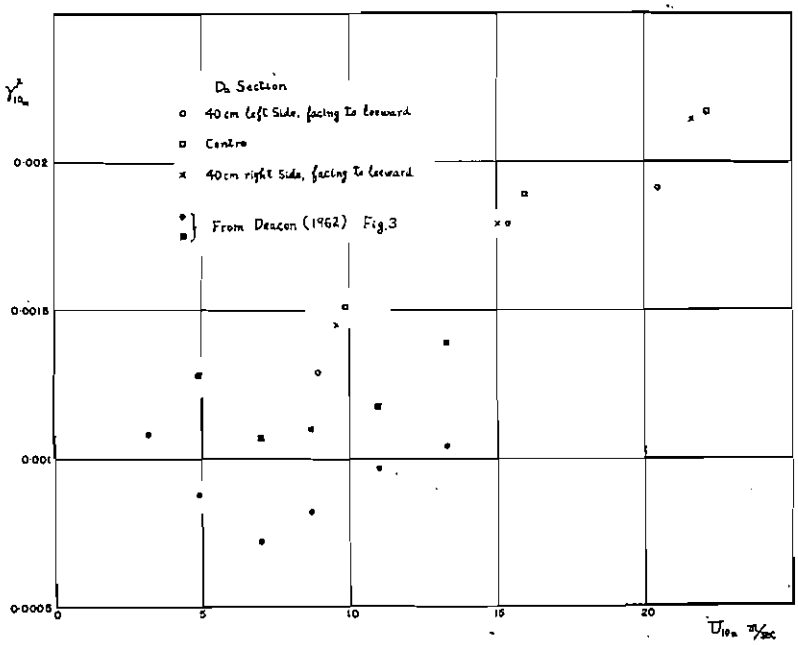

Fig-16 γ^2_{10m} related to U_{10m}

change of γ^2_{10m} against U_{10m} is consistent. In Fig-16 γ^2_{10m} from our experiment and E. L. Deacon's paper are shown, and it suggests that the increase of γ^2_{10m} subsequent to wind velocity U_{10m} may be a result of properties of turbulent boundary layer of air flow on water surface in the range of wind velocity considered. The physical meaning of τ_0 will be reexamined in 3—8 in relation to the energy spectrum of wavy surface.

Fig-17 is the relation of z_0 to U_*^2 as the air flow is assumed to be a fully developed rough flow. Although it contains some problems remained, the general relation is $z_0 \sim 2\times10^{-5}\, U_*^2$. According to J. W. Miles (1960). Ω in this case is about 3×10^{-3}, and z_0 is relatively small when it is compared with some observed result in actual ocean (T. H. Ellison (1956)).

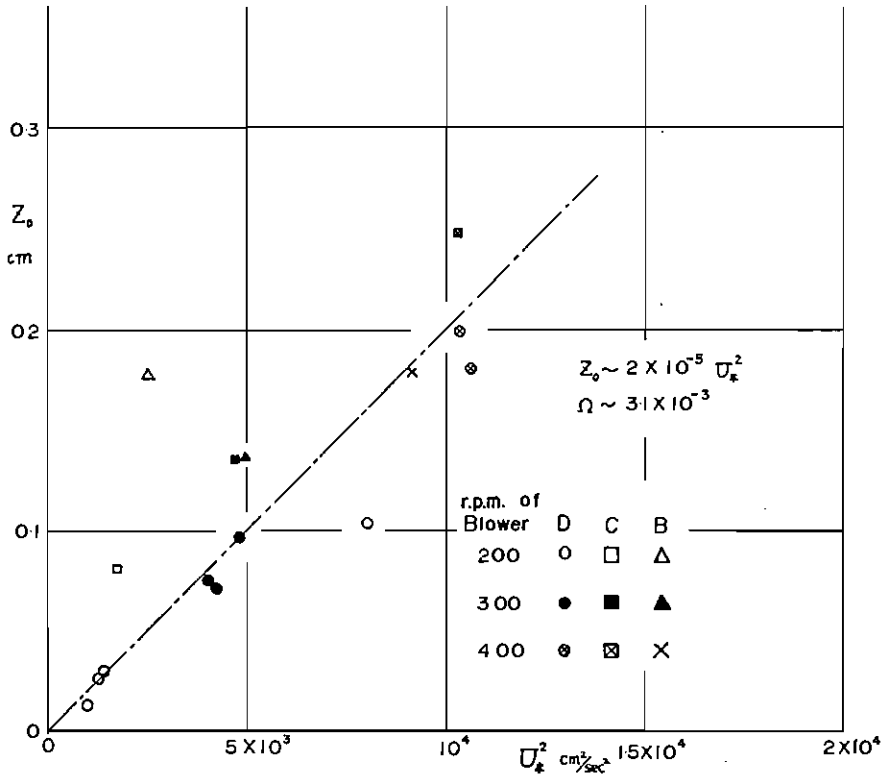

Fig-17 Z_0 related to U_*^2

3-4 Wind wave spectrum obtained

Fig-18 indicates the energy spectrum of wave profile at the centre of B_w, C_w and D_w Cross Section in the condition of 200 r.p.m. of blower (average wind velocity through the cross section at A_a Cross Section is 5.60 m/sec.). Fig-19 and 〃-20 correspond to 300 r.p.m. of blower and 400 r.p.m. of blower respectively. In these spectrum representations, nonlinear components (L. J. Tick (1959)) are perceived conspicuously in their high frequency range. This is strengthened in a case of 400 r.p.m. of blower as is stated in 2—3.

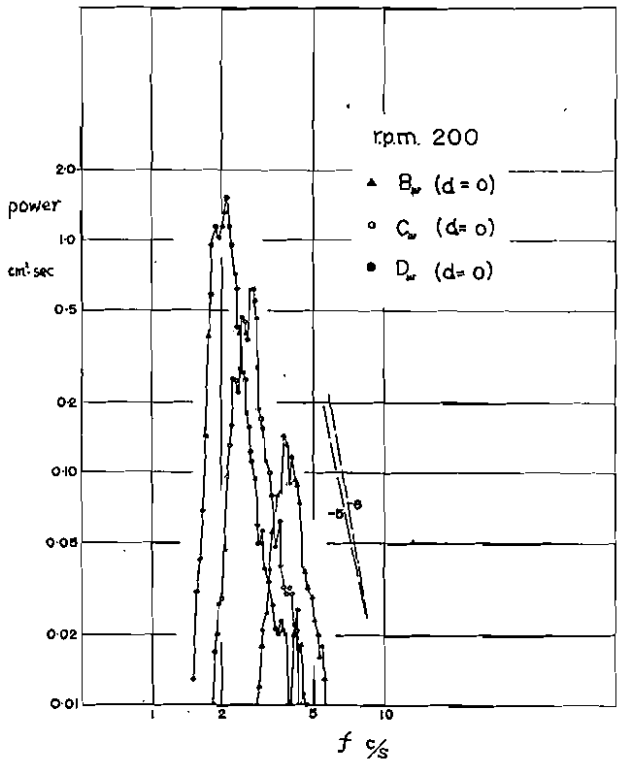

Fig-18 Spectrums of Wave Profile, r.p.m. of Blower 200

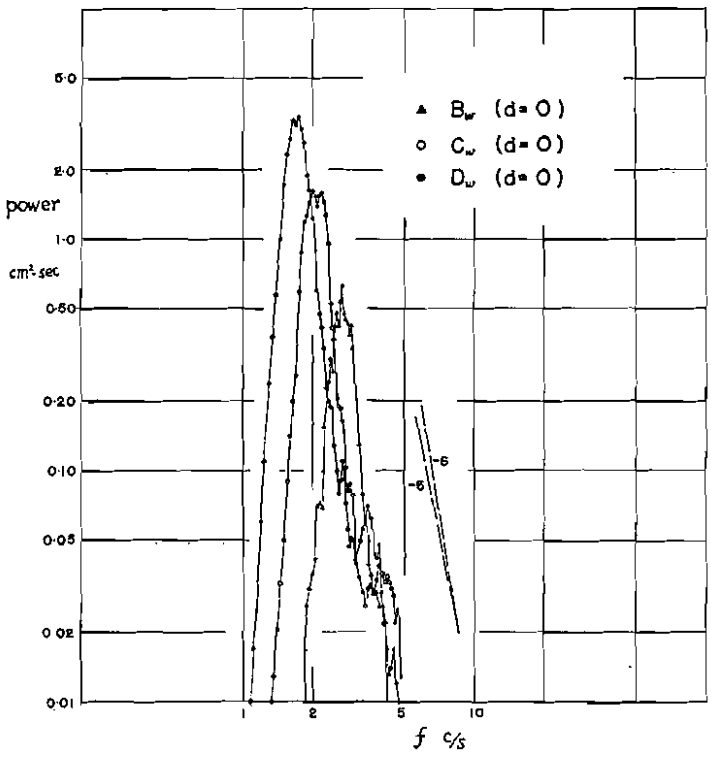

Fig-19 Spectrums of Wave Profile, r.p.m. of Blower 300.

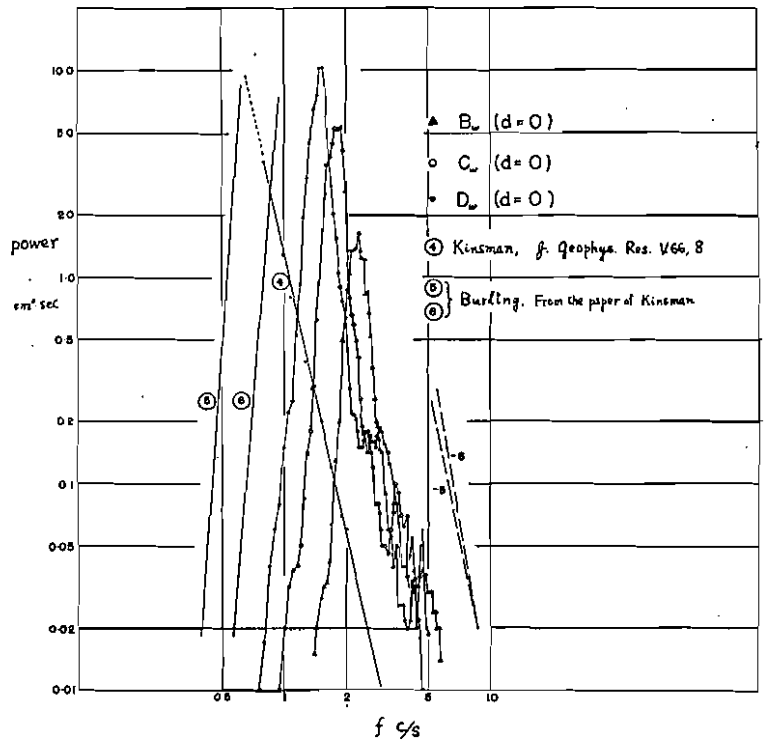

Fig-20 Spectrums of Wave Profile, r.p.m. of Blower 400.

But in the analysis of this experiment we use the linear theory except for cases when nonlinearity plays predominant roles, and stillmore, following to L. J. Tick (1959), gaussian assumption is used.

According to D. E. Cartwright and M. S. Longuet-Higgins (1956) W. J. Pierson, Jr. (1954) and S. O. Rice (1944, 1945), $\overline{f}$ zero up cross, $\overline{\overline{T}}$, $\overline{f}$ Max. and f (at peak of spectrum) are computed and shown in Table-4. Concerned to wave frequencies, the relation of f (at peak of spectrum) $< \overline{f}$ zero up-cross $< \overline{f}$ Max is consistent in every case, and

Table-4 Characteristics of Wind Waves

Section	r.p.m.of Blower	$\overline{f}$ zero up-cross	$\overline{\overline{T}}$ sec	$\overline{f}$ Max.	f (peak of spectrum)	ε	$\frac{f \text{ (peak of spectrum)}}{\overline{f} \text{ zero up-crose}}$
B_w	200	4.03	0.248	4.22	3.70	0.295	0.918
B_w	300	2.78	0.359	3.01	2.70	0.389	0.971
B_w	400	2.58	0.387	3.12	2.30	0.562	0.891
C_w	200	2.76	0.362	2.92	2.65	0.324	0.960
C_w	300	2.26	0.442	2.58	2.10	0.479	0.929
C_w	400	1.95	0.512	2.27	1.85	0.512	0.948
D_w	200	2.24	0.446	2.53	2.10	0.460	0.937
D_w	300	1.90	0.526	2.24	1.75	0.529	0.921
D_w	400	1.71	0.584	2.26	1.55	0.653	0.906

$\frac{f_{(\text{at peak of spectrum})}}{\bar{f}_{\text{zero up-cross}}}$ is about 0.9a nd almost constant. Concerned to ε, which indicates the band width of spectrum, ε generally increases with the development of waves. Table-5 shows $\overline{\eta^2}=\int_0^\infty E(\omega)\,d\omega$ and $H_{1/3}$ computed by the method of M. S. Longuet-Higgins (1952) ($\varepsilon\to 0$).

Table-5 Characteristics of Wind Waves

Section	r.p.m. of Blower	$\overline{\eta^2}$ cm^2	$\sqrt{\overline{\eta^2}}$ cm	$H_{1/3}$ cm
B_w	200	0.149	0.386	1.546
B_w	300	0.409	0.640	2.562
B_w	400	1.006	1.002	4.012
C_w	200	0.381	0.617	2.470
C_w	300	1.052	1.026	4.108
C_w	400	2.431	1.559	6.242
D_w	200	0.751	0.867	3.472
D_w	300	1.756	1.325	5.306
D_w	400	3.708	1.925	7.708

Then we examined the translation celerities of wave profiles which were moving to leeward. Moving pictures of these wind waves were taken through the glass side wall setting C_w Cross Section to the centre of picture and the times required by the passage of appeared wave crests during the distance of 50 cm and 100 cm were pursued. In some cases, wave crest disappeared away, and even in cases when wave profile sustained its shape varied roughly and the time required was random. But in cases when wave crest did not disappear, the average value of celerities of about 20 observations was computed and Table-6 shows the results. The reason is not clear why the celerities measured in a distance of 100 cm are greater than in a distance of 50 cm. A noticeable point is that averaged translation celerity of appeared wave crest is very near to the wave celeritry computed by the linear surface wave theory

Table-6 Translation Celerity of Wave Crest at C_w Section

r.p.m. of Blower	Translation celerity (1) cm/sec	〃 (2) cm/sec	$C=\frac{g}{2\pi}\frac{1}{f}$ (3) cm/sec	〃 (4) cm/sec
200	58.21	64.17	56.48	58.83
300	71.15	74.19	68.98	74.23
400	81.64	84.15	79.94	84.27

(1) Between the length of 50 cm
(2) 〃 100 cm
(3) f is saken to $\bar{f}$ zero up-cross
(4) f is taken to f (peak of spectrum)

by making use of $\bar{f}_{\text{zero up-cross}}$ and $f_{\text{(by peak of spectrum)}}$ as the representative wave frequencies. It seems a simple experimental support for the approximate use of linearized irrotational theory in the problem of development of wind waves.

3-5 Some characteristics of wave spectrums

We have not yet found the published paper which described the developing surface wave spectrum in the experimental air-water tunnel, and the published data by R. W. Burling (1959) and B. Kinsman (1961) are related to the field observation in the pond of short fetch. Wind velocities in their observations are relatively small (less than 10m/sec. at the height of 10 m above water surface) and their fetches are from several hundred metres to about 3 kilometres.

Here we compare our experimental spectrums in Fig-18, 〃-19 and 〃-20 with spectrums of R. W. Burling and B. Kinsman. The f^{-5} law (O. M. Phillips (1958)) as the high frequency equilibrium is relatively agreeable with the data of R. W. Burling and B. Kinsman. But in our data at the zone of high frequency which is inclusive of nonlinear effect the intensity of spectrum is alike to the law in average, and from this zone to the peak of spectrum the shape of spectrum is steeper than the f^{-5} law in every case. Straight lines indicative of slopes of f^{-5} and f^{-6} in each figures of Fig-18, 〃-19 and 〃-20 and a line of $f^{-4.5}$ in Fig-19, which is rewritten from Fig-5 of B. Kinsman (1961), all suggest clearly this different character of our data.

Some interpretations of the equilibrium condition $g^2 f^{-5}$ was given by W. J. Pierson, Jr. (1959). In our case, we suggest that this equilibrium condition is the condition of very weak (almost linear) equilibrium, because the spectrum intensity is given by $E(f) \sim g^2 f^{-5}$ and this expression means that the intensity is independently determined by local frequency. In Fig-19, in the zone of high frequency there is a domain which is plainly influenced by nonlinear effect and, although it is in a narrow region, $E(f) \sim f^n (n \geqq o)$ is exposed. In this region of strong nonlinear effect, the spectrum intensity is influenced by the intensity of regions near spectrum peak through nonlinear interaction (L. J. Tick (1959)), and is not thoroughly determined by the local frequency. The law $g^2 f^{-5}$ may be inconsistent in this region.

The existence of steeper slope than f^{-5} in the area from the spectrum peak to the above-mentionel region is due to the fact that the equilibrium condition is not established here. It means that, if we fix our eyes upon each frequency component, the wave energy lost by the breaking and other dissipative mechanism is greater than the energy given by air flow to wave. If this is permissible, our experiment of extremely small c/U_1 will show the different high frequency spectrum from those of Burling and Kinsman. Of course the truth may not be so simple and the breaking may cause a strong interfere of wave energy of different frequencies, and, as O. M. Phillips (1960) presented, interaction in a sense of finite amplitude wave exists.

Then we examine the relation of the intensity of spectrum peak to its frequency in Fig-18, 〃-19 and 〃-20. Fig-21 shows the result, and in this figure $E(f)$ at the peak of the spectrum moves along $f^{-4.2}$ (200 r.p.m. of blower), $f^{-3.5}$ (300 r.p.m. of blower) and $f^{-4.0}$ (400 r.p.m. of blower). These are all indicative that $E(f)$ at the peak does not move along f^{-5} curve, and rather it has a tendency of slowly varying. Comparing this result with the tendency of rapid variation along steeper slope than f^{-5} in the high frequency zone of spectrum, it seems very interesting and future studies may be necessary. In Fig-1 of O. M. Phillips (1958), this tendency was not so explicit.

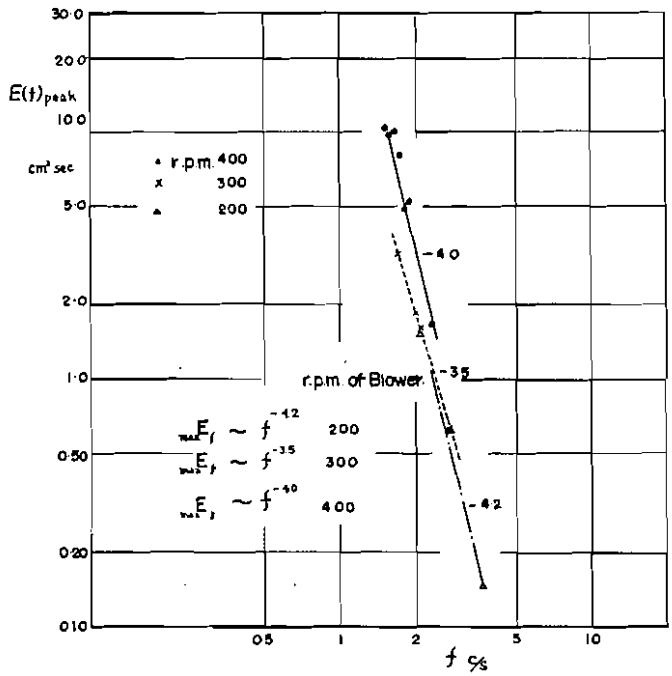

Fig-21 The intensity of spectrum at the peak related to its frequency.

Concerned to the agreement of our result with those of Burling and Kinsman in the zone of low frequency (so called developing range), we rewrite into Fig-20 two representative lines, which are selected from many lines of $E(f)$ in developing range in Fig-2 of B. Kinsman (1961). The slope of these two curves are agreeable with ours.

3-6 Comparison of our data with S-M-B curves

In the same way of fetch graph in S-M-B method, $\frac{gH_{1/3}}{U^2}$ and $\frac{g\bar{\bar{T}}}{2\pi U}$ are ralated to $\frac{gF}{U^2}$ in Fig-22 (—1, 2) and Fig-23 (—1, 2). U is taken actually at 40 cm high the mean water level in one side of the figures, and in another side of the figures U is assumed from the logarithmic profile at 1000 cm high above the same level. In both cases the velocity is averaged in B_a, C_a and D_a Cross Section. Recorded points

in these figures include the measurements of C_w-1, C_w-2 and C_w-3 Cross Section in addition to those of B_w, C_w and D_w Cross Section. In these two figures, if we take U_{10m} as U, $\frac{gH_{1/3}}{U^2}$ and $\frac{g\bar{\bar{T}}}{2\pi U}$ of ours situate lower than the S-M-B curves (C. L. Bretschneider (1958)), and, if U_{40cm} is taken as U, our results are relatively near to S-M-B curves. Accordingly, the determination of height at which the wind velocity is measured is still a problem, and at the same time it must be noted in this experiment z_0 against to U_* is fairly small in comparison with those in the actual ocean.

In Fig-22 the distribution of our experimental value indicates that $\frac{gF}{U^2}$ as a lateral abscissa is not a sufficient parametre to controll the development of wind waves. Actually, refering to the complicated propertics of non-negative damping factor of waves, this simple expression is not satisfactory.

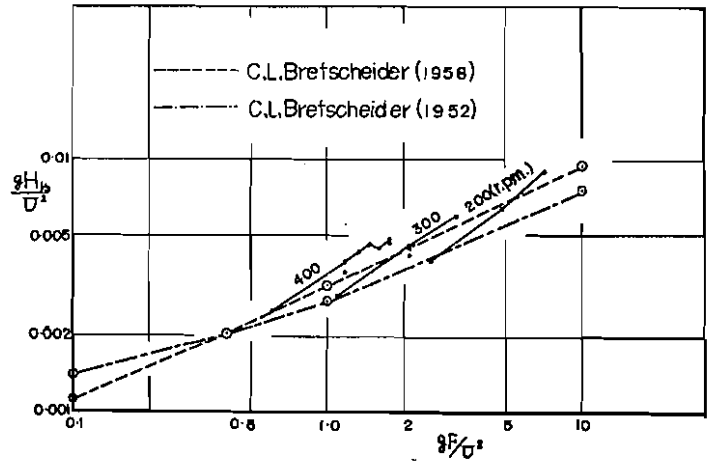

Fig-22-1 $\frac{gH_{1/3}}{U^2}$ related to $\frac{gF}{U^2}$

U is taken at the height of 40 cm above mean water level.

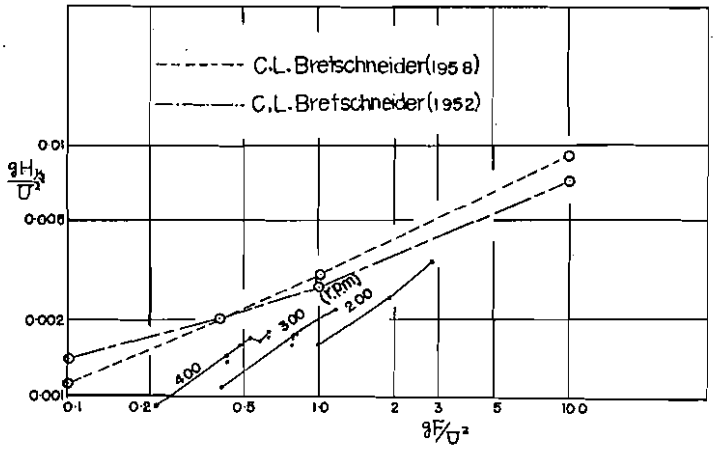

Fig-22-2 $\frac{gH_{1/3}}{U^2}$ related to $\frac{gF}{U^2}$

U is taken at the height of 1000 cm by the logarithmic profile.

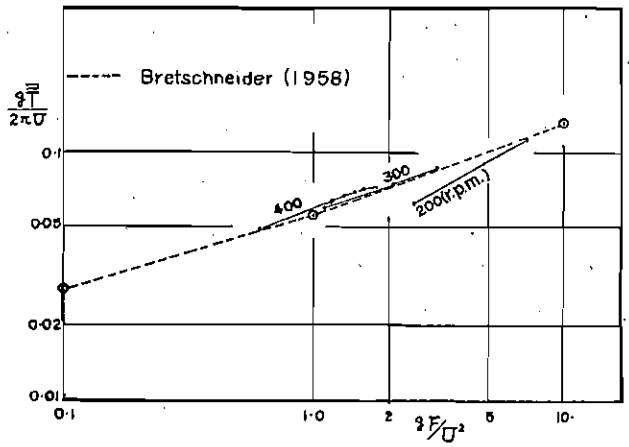

Fig-23-1 $\frac{g\,\overline{\overline{T}}}{2\pi U}$ related to $\frac{g\,F}{U^2}$

U is taken at the height of 40 cm above mean water level.

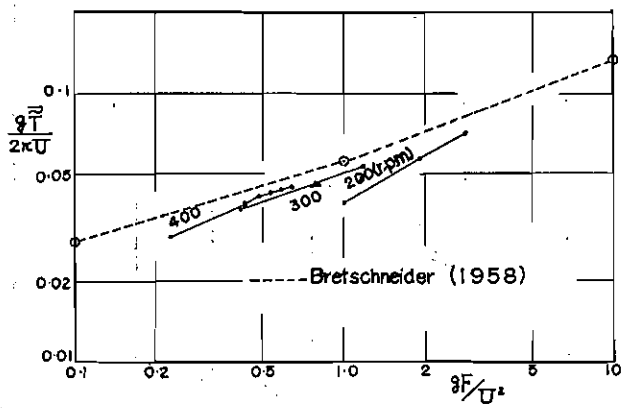

Fig-23-2 $\frac{g\,\overline{\overline{T}}}{2\pi U}$ related to $\frac{g\,F}{U^2}$

U is taken at the height of 1000 cm by the logarithmic profile.

3-7 Determination of non-negative damping factor by the data of wave development

We limit the computation to the linearized small amplitude wave, which includes the effect of molecular viscosity. Wind waves in this experiment can be generally treated as deep water waves. In the surface condition of waves, variation of normal stress of air flow and oscillatory shearing stress along the surface are considered. For the case when the surface condition is calm, H. Lamb (1932) gives the solution.

Equations of motion are

$$\frac{\partial u}{\partial t}=-\frac{1}{\rho}\frac{\partial p}{\partial x}+\nu\nabla_1^2 u \qquad (1)$$

$$\frac{\partial v}{\partial t}=-g-\frac{1}{\rho}\frac{\partial p}{\partial y}+\nu\nabla_1^2 v \qquad (2)$$

Equation of continuity is

$$\frac{\partial u}{\partial x}+\frac{\partial v}{\partial y}=0 \qquad (3)$$

Here we put

$$u=-\frac{\partial \varphi}{\partial x}-\frac{\partial \psi}{\partial y},\quad v=-\frac{\partial \varphi}{\partial y}+\frac{\partial \psi}{\partial x}$$

$$\text{and}\quad \frac{p}{\rho}=\frac{\partial \varphi}{\partial t}-\mathrm{g\,y} \qquad (4-1,\ 2,\ 3)$$

and so

$$\nabla_1^2\varphi=0,\quad \frac{\partial \psi}{\partial t}=\nu\nabla_1^2\psi \qquad (5-1,\ 2)$$

Surface conditions and

$$\mathrm{v}=\frac{\partial \eta}{\partial t} \qquad (6-1)$$

$$T\frac{\partial^2\eta}{2x^2}-p_a=-p+2\mu\frac{\partial v}{\partial y}=\rho g\eta-\rho\frac{\partial \varphi}{\partial t}+2\mu\frac{\partial v}{\partial y} \qquad (6-2)$$

$$(\tau_{xy})_a=\mu\left(\frac{\partial v}{\partial x}+\frac{\partial u}{\partial y}\right) \qquad (6-3)$$

(6—1, 2, 3) are receivable in the case of small amplitude wave. Bottom conditions are

$$\varphi,\ \psi\to 0 \qquad \text{at}\quad y=-\infty \qquad (7)$$

We put

$$\varphi=\int_{-\infty}^{\infty}e^{i(kx+nt)}d\xi_1\,(k,n,y) \qquad (8-1)$$

$$\psi=\int_{-\infty}^{\infty}e^{i(kx+nt)}d\xi_2\,(k,n,y) \qquad (8-2)$$

$$\eta=\int_{-\infty}^{\infty}e^{i(kx+nt)}d\xi_3\,(k,n) \qquad (8-3)$$

$$(\tau_{xy})_a=\int_{-\infty}^{\infty}e^{i(kx+nt)}\{N_1\,d\xi_3\,(k,n)+d\xi_4(k,n)\} \qquad (8-4)$$

$$p_a=\int_{-\infty}^{\infty}e^{i(kx+nt)}\{M_1\,d\xi_3\,(k,n)+d\xi_5(k,n)\} \qquad (8-5)$$

and, by making use of (5—1, 2), (6—1, 2, 3), $d\xi_n$ ($n=1, 2, \cdots, 5$) are eliminated. In this case $d\xi_4$, $d\xi_5$ have no physical meaning, and can be neglected. N_1 and M_1 are complex, and so they consist of both the quantities in phase of wave profile and in phase of wave slope. By making use of some conditions appropriate to the properties of the present wave problem, and after some abbreviations of higher order terms, the following algebraic equation may be obtained to the progressive wave (here $n=i\,n_1$)

$$n_1^3-4\nu k^2n_1^2+\left\{(gk+T'k^3)+\frac{k}{\rho}\left(M_1-\frac{N_1}{i}\right)\right\}n_1+2\nu k^2\frac{N_1}{\rho}\left(\frac{N_1}{\nu}\right)^{\frac{1}{2}}=0 \qquad (9)$$

This equation cannot be strictly solved. But in the present problem, as the first approximation, the first and the third terms in the left hand side are noticed, and we solve (9) as to these two terms. Inserting the approximate n_1, thus obtained into the second and fourth terms of the left hand side of (9), we obtain the solvable algebraic equation of n_1. The principal terms of the solution may be simplified as follows.

$$n=-\sigma_0-\frac{k}{2\rho\sigma_0}(M_1+i\,N_1)+i\,2\nu\,k^2 \tag{10}$$

$$\begin{cases} \text{have } g\,k+T'k^3=\sigma_0^2 \\ T/\rho=T' \end{cases}$$

Accordingly, if we take the spectrum for (8—3),

$$\phi(k)\,d\,k=\overline{e^{int}d\,\xi_3(k)\,(e^{int})^*\{d\,\xi_3(k)\}^*}$$

Putting $M_1=M_{11}+i\,M_{12}$, $N_1=N_{11}+i\,N_{12}$

$$\phi(k)\,d\,k=\overline{e^{\frac{k}{\rho\sigma_0}(M_{12}+N_{11})t}\,e^{-4\nu k^2 t}\,|d\,\xi_3(k)|^2} \tag{11}$$

$|d\,\xi_3(k)|^2$ indicates $\phi(k)\,d\,k$ at t=0.

If this method is simply approximated to the three-dimensional case,

$$\eta(X,t)=\int_{-\infty}^{\infty}e^{i(K\cdot X+n(K)t)}\,d\,\xi_3(K) \tag{12}$$

and

$$\phi(K)\,dk_1\,dk_2=e^{\frac{k}{\rho\sigma_0}(M_{12}(K)+N_{11}(K))t}\,e^{-4\nu k^2 t}\,|d\,\xi_3(K)|^2 \tag{13}$$

here $|K|=k \quad (\infty>k>0)$

We take k_1—axis along the direction of air flow, and use the relation $dk_1dk_2=kdkd\,\alpha$, and stillmore transform t as $t=\dfrac{F_e\,\sec\alpha}{\frac{c}{2}}$ (F_e : Fetch distance). Accordingly, the frequency spectrum in the present case is

$$E(\omega)=4\left\{\frac{\omega^3}{g^2}e^{\left\{s\frac{1}{c}\frac{g}{c^2}U_1^2\cos^2\alpha\cdot(m'_{12}(\omega)+n'_{11}(\omega))-4\nu\frac{\omega^4}{g^2}\right\}\frac{F_e\sec\alpha}{\frac{C}{2}}}\left(-\frac{\pi}{2}<\alpha<\frac{\pi}{2}\right)\right.$$
$$\left.\times\,\phi\,(\omega,\alpha)_{F_e=0}\,d\alpha\right. \tag{14}$$

have $\omega=2\pi f$, $s=\dfrac{\rho_a}{\rho}$ $\quad\begin{pmatrix}\rho_a : \text{density of air} \\ \rho \ : \text{density of water}\end{pmatrix}$

In the transformation of $M_{12}(K)+N_{11}(K)$ to $m'_{12}(\omega)+n'_{11}(\omega)$, we use the similar method to J. W. Miles (1957). In this expression the contribution of $N_{11}(K)$ is far smaller than that of $M_{12}(K)$.

If $\phi(\omega,\alpha)$ is substantially effective in $|\alpha|\leqq 20°$,

$$E(\omega)\fallingdotseq e^{\left\{s\frac{g}{c^3}U_1^2(m'_{12}(\omega)+n'_{11}(\omega))-4\nu\frac{\omega^4}{g^2}\right\}\frac{F_e}{\frac{c}{2}}}\int_\alpha\frac{4\omega^3}{g^2}\phi(\omega,\alpha)_{F_e=0}\,d\,\alpha$$
$$=e^{\left\{s\frac{g}{c^3}U_1^2(m'_{12}(\omega)+n'_{11}(\omega))-4\nu\frac{\omega^4}{g^2}\right\}\frac{F_e}{\frac{c}{2}}}E(\omega)_{F_e=0} \tag{15}$$

In (15) $m'_{12}(\omega)+n'_{11}(\omega)$ is the non-negative damping factor in this computation, and may be compared to the parametre β in J. W. Miles' computation (1957, 1960). In J. W. Miles' computation β is determined by his instability mechanism. In this experiment $m'_{12}(\omega)+n'_{11}(\omega)$ is computed by (15) from the frequency spectrum of surface waves, and so it may include both non-negative and negative components of damping factor. By making use of (15), we may compute $\{m'_{12}(\omega)+n'_{11}(\omega)\}$ at arbitrary fetch length and also at arbitrary frequency number.

Fig-24-1, 〃-2, 〃-3, 〃-4 and 〃-5 show the obtined $\{m'_{12}(\omega)+n'_{11}(\omega)\}$ by making use of the spectrum representations in Fig-18, 19 and 20. In the neighbouring points of the peak of the spectrum, $\{m'_{12}+n'_{11}\}$ is not derived. When wind waves progress in the fetch, $E(\omega)$ at the neighbouring points of the peak once increases and then decreases, and clearly $\{m'_{12}+n'_{11}\}$ at the same points of the spectrum cannot be considered to have values not so variable through the given length of the fetch.

General tendencies of the obtained values of $\{m'_{12}+n'_{11}\}$ are as follows; (i) $\{m'_{12}+n'_{11}\}$ is positive in the measured range from low frequency to the frequency of the peak of the spectrum, but the value decreases with the increase of frequency. (ii) The maximum value in the low frequency range is always greater than the computed value of β of J. W. Miles (1960). (iii) In the range of higher frequencies than that of the peak of spectrum, $\{m'_{12}+n'_{11}\}$ is almost always negative, but its absolute value is small and approaches to zero with the increase of frequency. (iv) $\{m'_{12}+n'_{11}\}$ in the low frequency side is greater in the fetch between C_w—D_w cross sections than in the fetch between B_w—C_w cross sections.

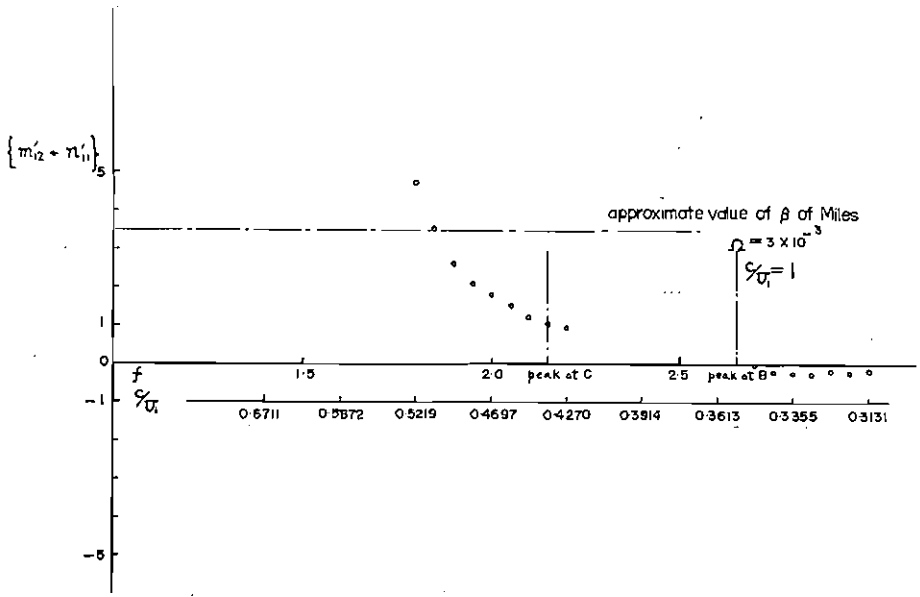

Fig-24-1 Values of $\{m'_{12}+n'_{11}\}$
Fetch between B_w and C_w sections, r.p.m. of Blower 300.

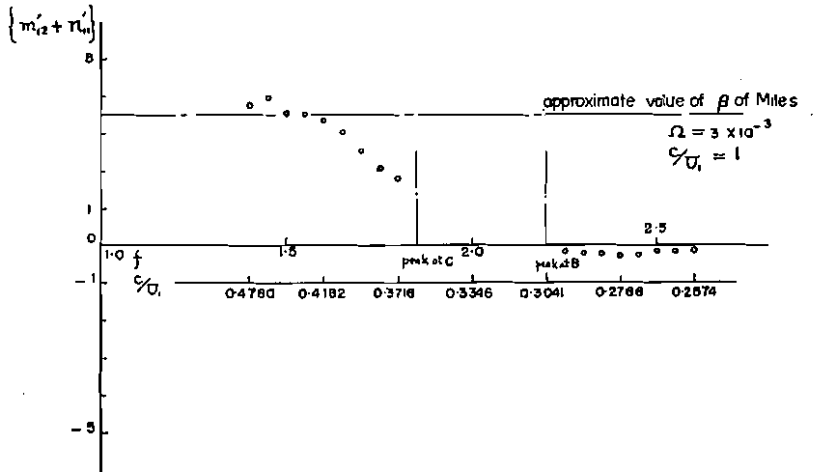

Fig-24-2 Values of $\{m'_{12}+n'_{11}\}$
Fetch between B_w and C_w sections, r.p.m. of Blower 400.

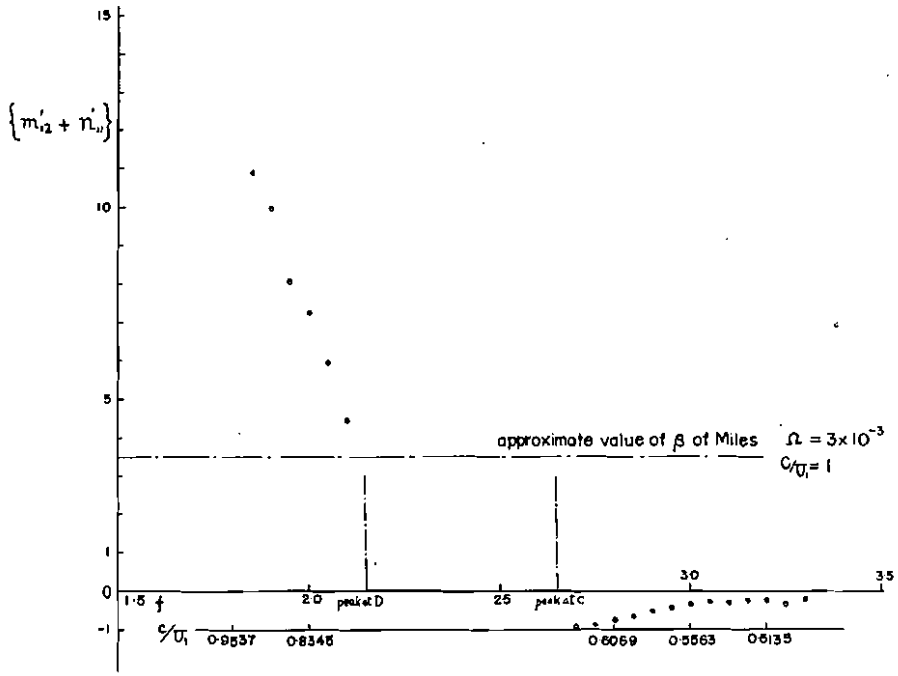

Fig-24-3 Values of $\{m'_{12}+n'_{11}\}$
Fetch between C_w and D_w sections, r.p.m. of Blower 200.

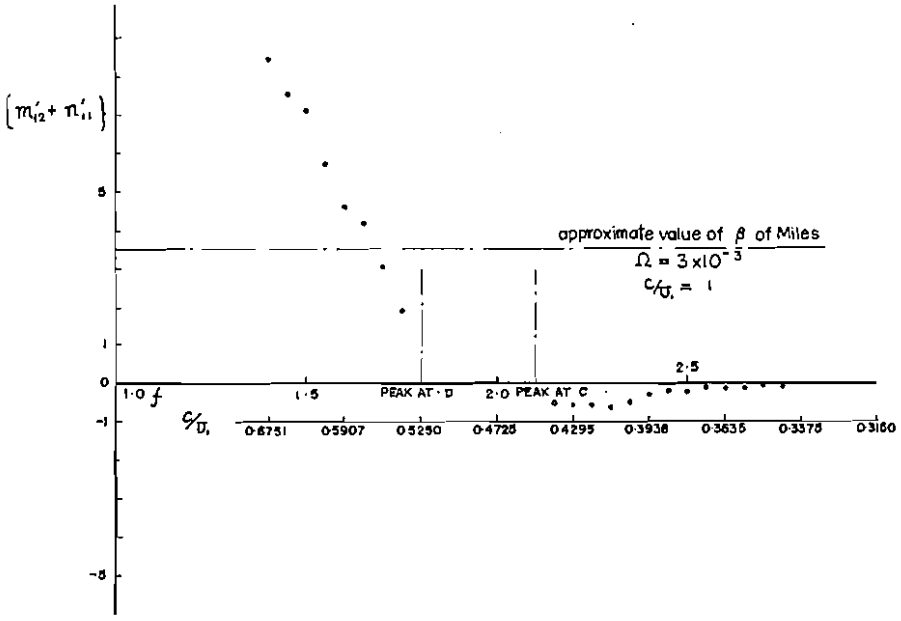

Fig-24-4 Values of $\{m'_{12}+n'_{11}\}$
Fetch between C_w and D_w sections, r.p.m. of Blower 300.

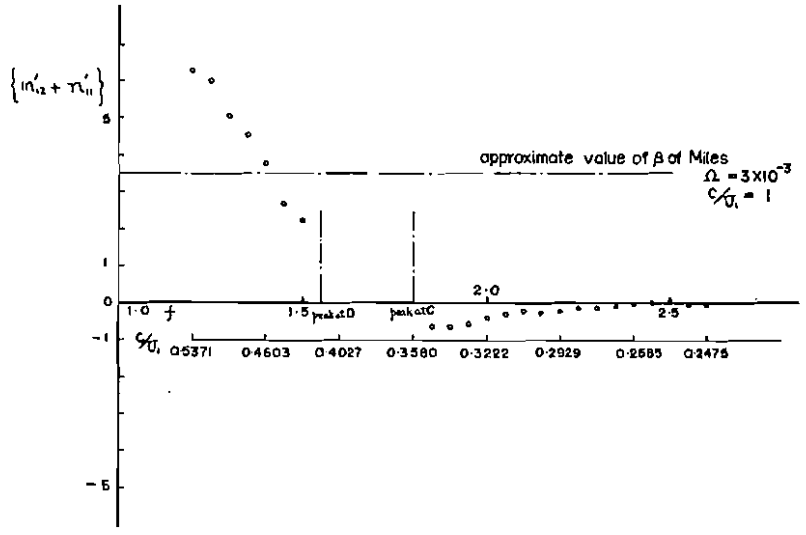

Fig-24-5 Values of $\{m'_{12}+n'_{11}\}$
Fetch between C_w and D_w section, r.p.m. of Blower 400.

The reason of the above mentioned property (ii) may be (ii-i) the difference of computation, (ii-ii) the influence of N_{11}, (ii-iii) the increase of non-negative damping factor by any other hydrodynamical causes than given by J. W. Miles. (ii-iii) may be explained as follows in this experiment, y_c, which satisfies $U \fallingdotseq c$, situates very near the water surface, and the viscous effect is very strong to increase the non-negative damping factor, and its effect may become comparable with the usual

effect of inviscid singularity. Still more in the presence of finite amplitude wave, phase shift effect in more general features may be caused because air flow cannot follow along wavy surfaces strictly. (ii-iii) may be probable in this experiment which was done in the condition of very small value of c/U_1, and sufficient high Reynolds number of air flow.

One more reasons of (ii) is the transfer of wave energy from the zone of high frequency to the low frequency zone. This energy transfer may be caused by the breaking and other nonlinear interactions.

The negative value of $\{m'_{12}+n'_{11}\}$ in the range of high frequencies may be resulted by the fact that the energy loss of waves due to breaking and other origins exceeds the supply of wave energy from air flow. In more detailed inspection, the value is small in the zone near the peak of the spectrum, and this small value of $\{m'_{12}+n'_{11}\}$ corresponds to the zone in which the intensity of spectrum varies with steeper slope than that is given by the f^{-5} law. In the zone of higher frequencies in which $\{m'_{12}+n'_{11}\}$ converges to zero, the intensity of spectrum has a distribution near to the f^{-5} law in average.

$\{m'_{12}+n'_{11}\}$ in the range of low frequencies obtained in the fetch between C_w—D_w cross sections becomes gradually small in accordance with the increase of revolution number of blower. This tendency of non-negative damping foctor is consistent with the change c/U_1. In this experiment c/U_1 is extremely small, and in inverse to usual cases, non-negative damping factor becomes small with the decrease of c/U_1. In the paper of J. W. Miles (1960), β is related to ξ_c $(=k\,y_c)$ with the assumption of logarithmic profile of wind velocity. If we compute ξ_c in our cases, the variation of β related to ξ_c has a same tendency with $\{m'_{12}+n'_{11}\}$, but the variation of $\{m'_{12}+n'_{11}\}$ is far great. At this point separation of air flow from wave profile of three-dimensional finite amplitude should be taken into account.

$\{m'_{12}+n'_{11}\}$ in the range of low frequencies becomes smaller in the fetch of B_w—C_w cross sections than in the fetch of C_w—D_w cross sections. This relation is inverse to the change of $z_0/H_{1/3}$, and may be linearly explained by $\beta\sim\xi_c$ $(=k\,y_c)$ relation of J. W. Miles (1960). In this experiment $H_{1/3}$ equals to $(0.11\sim0.17)\ \bar{\bar{L}}$ ($\bar{\bar{L}}$ means the wave length that corresponds to $\bar{\bar{T}}$), and this indicates that the waves may be considered to be extremely steep. $z_0/H_{1/3}$ is linearly related to z_0/c^2. Thus the increase of ξ_c explains the decrease of $\{m'_{12}+n'_{11}\}$ in a shape of β. But even in this case wind profile may act another effect on the extremely steep waves under the condition that c/U_1 is very small. As already shown, in the fetch of B_w—c_w cross section the turbulent boundary layer of air flow along the water surface is not sufficiently developed. Accordingly, the fact that z_0 is comparatively large there in contrast with $H_{1/3}$ may be interpreted to index that the separation of stream line along wavy surface is large. In this case, the intensity of perturbed flow of J. W. Miles is

weakened and β becomes small.

3-8 Some problems related to non-negative damping factor

Components of τ_0 that is deduced from logarithmic assumption of velocity profile and is shown in Table -1, 2 of 3-3 may be divided into (i) surface shear given by molecular viscosity of air flow, (ii) phase shift effect of wall friction layer upon normal stress due to molecular viscosity, (iii) hydrodynamical effect of critical point (y_c) shown by J. W. Miles (1957) and interpreted physically by M. J. Lighthill (1962), (iv) phase shift effect that is appeared when the stream line of air flow on water surface does not follow the wavy surface strictly.

The effects of (ii), (iii) and (iv) are included to τ_0 as $\frac{1}{2}\overline{R\left\{p_a\left(\frac{\partial\eta}{\partial x}\right)^*\right\}}$, and so normal pressure in phase with the surface slope of wavy surface is effective. In this treatment, the phenomenon, that the stream line of air does not follow the wavy surface strictly, has two physical meanings. At first, in the treatment of J. W. Miles (1957) perturbed flow ϕ may decrease by this separation, and β may decrease. Secondly this phenomenon may cause the phase shift of air flow from the wavy surface, and in short some part of α in J. W. Miles (1957) may be transferred to the part of β. This may generally increase β. (The phase of perturbed flow ϕ may be somewhat shifted from the computation of J. W. Miles.)

Accordingly, both the case when non-negative damping factor decreases and the case when that increases may be allowable. For example, as c/U_1 is very small in our experiment, non-negative damping factor for short small waves among the long great waves may decrease because the perturbed flow ϕ against them may decrease. For long great waves, the non-negative damping factor may increase or decrease in accordance with the degree of wave height, the magnitude of c/U_1 etc..

As the air flow in this experiment is very near to the fully developed rough flow, the effect of surface shear given by molecular viscosity of air flow upon τ_0 seems small. If we neglect this effect and introduce the parametre β', which is the coefficient of fluctuation of normal pressure in phase with the surface slope of wavy surface and is assumed to be constant in the considered domain of wave frequencies, a simple computation shows

$$\tau_0=\frac{1}{2}\overline{R\left\{p_a\left(\frac{\partial\eta}{\partial x}\right)^*\right\}}=\int_{f_1}^{f_2}\beta'\rho_a U_1^2\frac{16\pi^4 f^4}{g^2}E(f)\,df \tag{16}$$

In the case when the nonlinear component of $E(f)$ is considered as the second perturbed component of L. J. Tick (1959), the simplest approximation is

$$\tau_0=\int_{f_1}^{f_2}\beta'\rho_a U_1^2\frac{16\pi^4 f^4}{g^2}E_l(f)\,df+\int_{f_1}^{f_2}\beta'\rho_a U_1^2\frac{n\pi^4 f^4}{g^2}E_n(f)\,df \tag{17}$$

Here $E_l(f)+E_n(f)$ equals $E(f)$, $E_l(f)$ is the linear part of $E(f)$ and $E_n(f)$ is the nonlinear part of $E(f)$. When there is one spike spectrum, $E_n(f)$ appears at the

twofold frequeneies of $E_t(f)$ and n in (17) may be put to 4. In the actual case, the accurate division of $E_t(f)$ and $E_n(f)$ is impossible, and so it stays within the estimation of degree.

Table-7 shows β' computed by (16) and (17). When (16), (17) are applied to the whole zone of spectrum, β' becomes smaller than $\{m'_{12}+n'_{11}\}$ in 3-7, and when (16) is applied to the zone of lower frequencies than that of the peak of spectrum, β' becomes larger than $\{m'_{12}+n'_{11}\}$. As n'_{11} is not so effective, β' has the almost same meaning as $\{m'_{12}+n'_{11}\}$. τ_0 in (16) is actually contains the effect of vicous shear, and so β' from (16) may be a little greater than its real value. Summarizing these considerations, a conclusion is proposed that the true non-negative damping factor originated by air flow gradually decreases from the zone of low frequency to the zone of high frequency (within the range of estimation of this experiment). Fig-25 is a schematic representation of the distribution of non-negative damping factor, which is discussed in this and the preceding paragraphs.

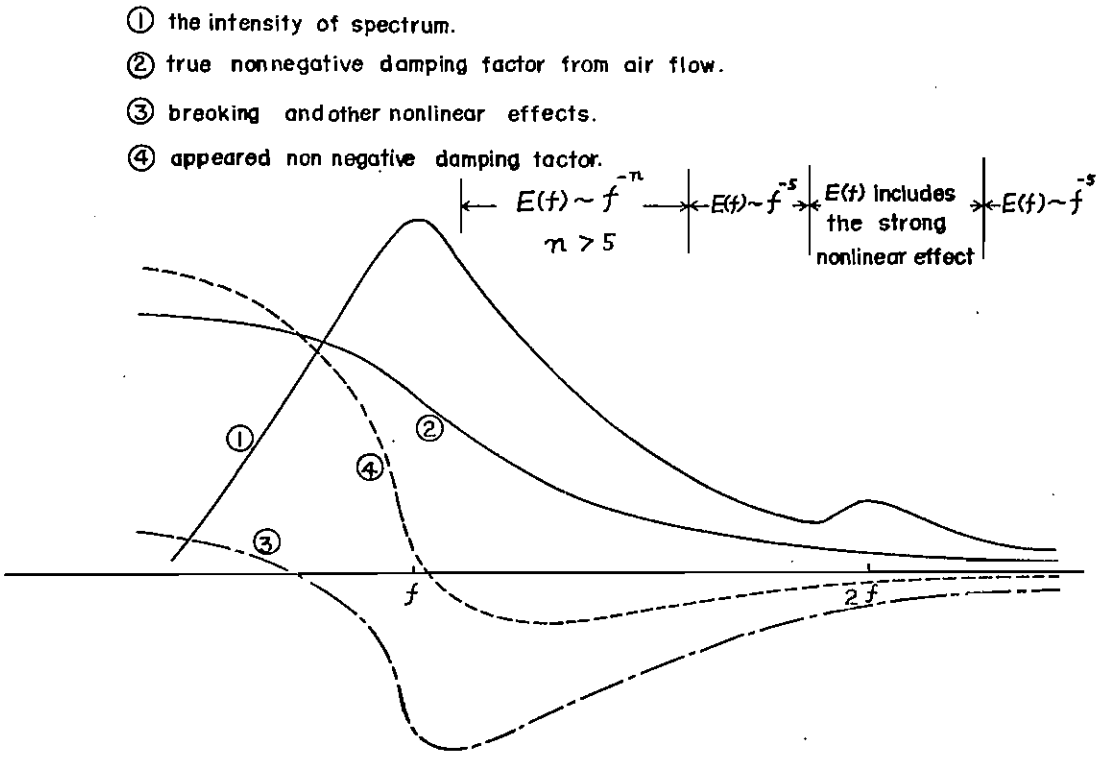

Fig-25 Schematic representation of non-negative damping factor.

Table-7 The value of β' from the Shearing Stress

Section	r. p. m. of Blower	$\beta'^{(1)}$	$\beta'^{(2)}$	$\beta'^{(3)}$	f peak of spectrum
B_w	200	——	——	——	3.70
C_w	200	4.075	4.306	14.44	2.65
D_w	200	4.193	5.013	15.39	2.10
B_w	300	3.442	3.744	12.52	2.70
C_w	300	2.702	3.083	13.06	2.10
D_w	300	3.016	3.480	19.20	1.75
B_w	400	1.509	1.811	9.54	2.30
C_w	400	2.112	3.373	10.46	1.85
D_w	400	1.743	2.243	13.78	1.55

(1) Equation (16) is used and $E(f)$ is taken to the whole spectrum.
(2) Equation (17) is used, $E(f)$ is taken to the whole spectrum, ands n is taken to 4.
(3) Equation (16) is used, and $E(f)$,is taken from the end of the lowest frequency to the peak of the spectrum.

Authors thank to Dr. H. Mitsuyasu for his help in the preparation of distribution graphs of 2—3.

References

Benjamin, T. B. 1959 Shearing flow over a wavy boundary, J, Fluid. Mech. Vo. 6.

Bretschneider, C. L. 1958 Revisions in Wave Forecasting: Deep and Shallow Water, Proc. 6 th confere. on Coastal Eng.

Burling, R. W. 1959 The Spectrum of Waves at Short Fetches, Dt. Hydrogr. Z., Band 12, Heft 2, 3.

Cartwright, D. E. and Longuet-Higgins, M. S. 1956 The statistical distribution of the maxima of a random function, Proc. Roy. Soc. A, Vol. 237.

Chang, S. S. 1955 A Magnetic Tape Wave Recorder and Energy Spectrum Analyzer for the Analysis of Ocean Wave Records, B. E. B. Tech. Memo., No. 58.

Darbyshire, J. 1959 A Further Investigation of Wind Generated Waves, Dt. Hydrogr. Z. Band 12, Heft. 1.

Deacon, E. L. 1962 Aerodynamic roughness of the sea, J. Geophys. Res. Vol. 67, No. 8.

Ellison, T. H. 1956 Atmospheric turbulence, Surveys in Mechanics, Cambridge Univ. Press.

Jeffrys, H.	1925	On the formation of water waves by wind, Proc. Roy. Soc. A. Vol. 107.
Jeffrys, H.	1926	On the formation of water waves by wind (second paper), Proc. Roy. Soc. A. Vol. 110.
Kinsman, B.	1961	Some Evidence on the Effect of Nonlinearity on the Position of the Equilibrium Range in Wind-Wave Spectra, J. Geophys. Res. Vol. 66, No. 8.
Lamb, H.	1932	Hydrodynamics, 6 th ed., Cambridge Univ. Press.
Lighthill, M. J.	1962	Physical interpretation of the mathematical theory of wave generation by wind, J. Fluid Mech. Vol. 14.
Longuet-Higgins, M. S.	1952	On the statistical distribution of the heights of sea waves, J. Mar. Res., Vol. 11.
Miles, J. W.	1957	On the generation of surface waves by shear flows, J. Fluid Mech. Vol. 3.
Miles, J. W.	1959	On the generation of surface waves by shear flows : Part 2, J. Fluid Mech. Vol. 6.
Miles, J. W.	1960	On the generation of surface waves by turbulent shear flows, J, Fluid Mech. Vol. 7.
Miles, J. W.	1962	On the generation of surface waves by shear flows, Part 4., J. Fluid Mech. Vol. 13.
Motzfeld, H.	1937	Die turbulente Strömung an welligen Wanden, Z. A. M. M. Band 17.
Phillips, O. M.	1957	On the generation of waves by turbulent wind, J. Fluid Mech. Vol. 2.
Phillips, O. M.	1958	The equilibrium range in the spectrum of wind-generated waves, J. Fluid Mech. Vol. 4.
Phillips, O. M.	1960	On the dynamics of unsteady gravity waves of finite amplitude, Part. I. The elementary interactions, J. Fluid Mech. Vol. 9.
Pierson Jr., W. J.	1954	An Electronic Wave Spectrum Analyzer and its Use in Engineering Problems, B. E. B. Tech. Memo., No. 56.
Pierson Jr., W. J.	1954	An interpretation of the observable properties of 'sea' waves in terms of the energy spectrum of the gaussian record, Trans. A. G. U., Vol. No. 5.
Pierson Jr., W. J.	1959	A note on the growth of the spectrum of wind generated gravity waves as determined by non-linear considerations, J. Geophys. Res., Vol. 64, No. 8.
Rice, S. O.	1944, 1945	The mathematical analysis of random noise. Bell. Syst. Tech. J. 23 and 24.

Stereo Wave Observation Project	1957	The directional spectrum of a wind generated sea, New York Univ.
Stewart, R. W.	1961	The wave drag of wind over water, J. Fluid Mech. Vol. 10.
Tick, L. J.	1959	A non-linear random model of gravity waves I, J. Math. Mech., Vol. 8, No. 5.

港湾技術研究所欧文報告 No.2

1963年6月

編集兼発行人　運輸省港湾技術研究所

発行所　運輸省港湾技術研究所
横須賀市川間162

印刷所　株式会社 白泉社
東京都港区麻布霞町7